The Effects of Reforming Byproducts on PEM Fuel Cell Performance

by

Justin Thomas Craft

Department of Mechanical Engineering and Materials Science
Duke University

Date:_____

Approved:

_____
Nico Hotz, Supervisor

_____
Adrian Bejan

_____
Walter Simmons

Thesis submitted in partial
fulfillment of the requirements for the degree
of Master of Science in the Department of
Mechanical Engineering and Materials Science
in the Graduate School
of Duke University

2014

ABSTRACT

The Effects of Reforming Byproducts on PEM Fuel Cell Performance

by

Justin Thomas Craft

Department of Mechanical Engineering and Materials Science
Duke University

Date:_____
Approved:

_____
Nico Hotz, Supervisor

_____
Adrian Bejan

_____
Walter Simmons

An abstract of a thesis submitted in partial
fulfillment of the requirements for the degree
of Master of Science in the Department of
Mechanical Engineering and Materials Science
in the Graduate School
of Duke University

2014

Abstract

One of the main goals of the Thermodynamics and Sustainable Energy Laboratory at Duke University is to create a Hybrid Solar System (HSS). The HSS is to consist of four main processes: solar steam reformation, fuel cleaning via a preferential oxidation reactor (PROX), hydrogen storage, and a Proton Exchange Membrane Fuel Cell (PEMFC).

The key goal of this research is to determine whether it is feasible to run this PEMFC on the expected gas mixture from the solar steam reformer after it is cleaned by the PROX (75% H_2 and 25% CO_2) with no significant power loss and no long-term damage to the fuel cell catalyst.

Findings were that even if the gas mixture input to the PEMFC consisted of 30% carbon dioxide and 70% hydrogen, the PEMFC would continue to operate as if the flow were 100% hydrogen with no negative long term effects to the PEMFC.

The PROX was then added to the setup and the expected gas mixture (from the solar collector) was run through the system. The results demonstrated that if the PROX achieves the expected 100% conversion (removal of the carbon monoxide to the necessary level of < 10 ppm), the PEMFC should handle the expected cleaned flow as if it were 100% hydrogen.

The findings in this research provide validation of the overall concept of the HSS.

Contents

List of Tables

List of Figures

List of Symbols

A, B, & C	Constants of the Medium
CO	Carbon Monoxide Molecule
CO_2	Carbon Dioxide Molecule
e^-	Electron (-)
H_2	Hydrogen Molecule
H_2O	Water Molecule
H^+	Hydrogen Proton (+)
I	Current (Amp)
n	Quantity of the Substance (moles)
n_{CO2}	Molar Flow Rate of Carbon Dioxide (mol/min)
n_{H2}	Molar Flow Rate of Hydrogen (mol/min)
O_2	Oxygen Molecule
p	Pressure (Pa)
P	Power (watt)
p_{atm}	Atmospheric Pressure (mmHg)
P_{MAX}	Maximum Power
Pt	Platinum Molecule
Pt-CO_{ads}	Platinum Molecule with Adsorbed Carbon Monoxide Molecule
Pt-H_{ads}	Platinum Molecule with Adsorbed Hydrogen Molecule

p_{vp}	Saturation Vapor Pressure (mmHg)
R	Ideal Gas Constant (J / K*mol)
RH	Relative Humidity (%)
T	Temperature (K)
T_C	Cold Source Temperature (K)
T_H	Hot Source Temperature (K)
v	Volume (m^3)
V	Voltage (V)
V_{CO2}	Volumetric Flow Rate of Carbon Dioxide (ccm)
V_{H2}	Volumetric Flow Rate of Hydrogen (ccm)
X_{H2}	Ratio of Hydrogen within Gas Mixture (%)
η	Maximum Theoretical Efficiency (%)
η_{th}	Thermodynamic Efficiency (%)
ΔG	Change in Gibbs Free Energy (kJ / mol)
ΔH	Change in Enthalpy (kJ / mol)

Acknowledgements

I would like to thank Dr. Nico Hotz (my faculty advisor) and the T-SEL Laboratory staff, especially Titilayo Shodiya who provided guidance and in-depth knowledge of the PROX reactor. I am deeply grateful for my family, including Dr. John Simon and Olinda Simon, David and Beuna Craft, Dr. Elena Aandstad, and my loving wife Heidi Craft (thank you for not killing me during the course of this academic endeavor), who gave me love and support throughout this process. Finally, thank you to my son, Simon, whose arrival motivated me to begin this pursuit two years ago.

1. Introduction

Throughout history one fundamental truth has been seen: civilization is built and expanded through the amount of usable energy and the ability to transfer said energy [1]. Therefore the more energy that can be converted into a usable form and the more efficiently it can be delivered, the more capability there is to support population and its growth. This concept is such an ingrained idea that many modern eras are named after prominent energy types available at the time, such as the Industrial (Steam) Age and the Nuclear Era. Since population is always increasing, the demand for energy also increases. Currently most energy demands are being met by burning fossil fuels, primarily oil and coal. These fossil fuels are burned to generate heat, which is then converted into electrical energy through various processes. However, the supplies of fossil fuel sources are limited and will eventually run out. Therefore, other means of energy conversion are needed to supply the ever-growing energy demand. The next generation of energy conversion systems needs to be more efficient and be supplied by renewable sources. Currently the primary energy sources being researched to meet these demands are wind power, solar power, tidal harvesting, and fuel cells.

Fuel cells offer a very appealing solution to our energy crisis because the hydrogen needed for the energy conversion process is abundant and can be gathered from renewable sources, such as converting biofuel. Another reason fuel cells are

attractive is that hydrogen offers a very high energy density per mass when compared to other available fuel sources.

The concept for the fuel cell methodology was conceived by Sir William Grove in 1839, with his work demonstrating the potential to convert electrical energy from hydrogen and oxygen with a "gaseous voltaic battery" [3,30]. However, it was not until the 1960's that what is considered to be Proton Exchange Membrane Fuel Cells (PEMFC) were created by Grubb and Niedrach in the General Electric labs under a contract for the United States Navy [3]. These fuel cells were researched and produced for use in the Gemini space shuttle programs. The Gemini missions had a longer flight time than previous missions, making a traditional battery ill suited. The fuel cells that were used in these missions were the ancestors of the fuel cells used today; they could operate at higher temperatures and used liquid cooled hydrogen and oxygen for inputs. The liquid cooling requirement is not practical for most terrestrial uses of modern fuel cells because large amounts of energy are required to maintain those extreme states without the benefit of being in space.

The fuel cell concept is still used in space shuttles today, albeit no longer in the PEMFC form. The PEMFC methodology was largely unused, except in a few satellites, until the 1990's when the oil crisis began to take shape and the search for alternative renewable energies began [3]. Fuel cell methodology often boasts an efficiency rating of approximately 60%, which is superior to that of typical internal combustion engines

which are widely used today and generally have an efficiency rating of approximately 30% or lower [2].

Another advantage of fuel cells is that they have zero emissions; the only byproduct from the process is water and any unused gas products within the feed lines (what goes in and is unused will come out). Other appealing factors generally associated with fuel cells are: small size and light weight, minimal noise pollution, and economic and political advantages in terms of decreased foreign dependency [3].

1.1 What is a Fuel Cell?

The simplest definition of a fuel cell is that it is a device that converts chemical energy into electrical energy [2,3]. Electrical energy is obtained by converting the chemical energy from the reaction of hydrogen and oxygen when it is combined into water through reverse electrolysis. The three main parts of a fuel cell are: an anode catalyst where the hydrogen is added, a cathode catalyst where the oxygen is added, and an electrolyte separating the catalysts.

The hydrogen is added into the system on the anode side, where the catalyst splits the molecule and allows only the protons from the split hydrogen molecule to pass through the electrolyte to the cathode. The electrons from the split hydrogen molecule cannot pass directly through the electrolyte, resulting in a flow of electrons directed to the cathode through a separate completed closed circuit. This flow of electrons is the current being generated by the fuel cell, which can be used to power any device. Once

on the other side, the cathode catalyst splits the oxygen molecule. These split oxygen atoms and the previously split hydrogen protons from the electrolyte will bond with the electrons flowing through the closed circuit to form water and thus complete the cycle (refer to Figure 1). If the protons or the electrons from the hydrogen do not reach the cathode side, water does not form and no electrical energy is generated.

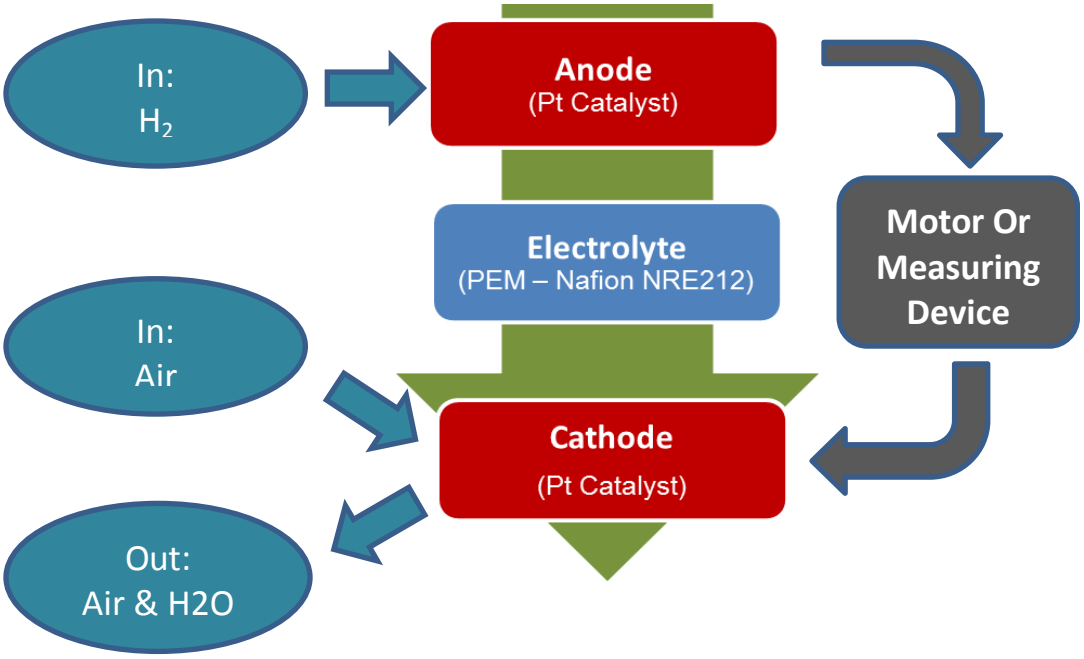

Figure 1: PEMFC Flowchart

The three parts are collectively referred to as the Membrane Electrode Assembly (MEA). The exact materials used in each of these three main parts vary among different classes of fuel cells. Examples of different classes of fuel cells are: Proton Exchange Membrane Fuel Cells (PEMFC), Phosphoric Acid Fuel Cells (PAFC), Solid Oxide Fuel Cells (SOFC), and several others. The electrolyte is usually the part that is altered

between different classes of fuel cells. Electrolyte materials can be composed of polymers, oxides, or acids. Changes to the anode or cathode catalyst are normally considered sub-classes of these fuel cell types. For example, in a simple PEMFC there could be a membrane comprised of only a platinum catalyst or there could be an alloy catalyst containing platinum, such as a platinum-ruthenium mixture, but the cell as a total unit would still be referred to as a PEMFC.

The different classes and sub-classes of fuel cells each have very distinct advantages and disadvantages associated with them. This paper focuses on a PEMFC type of fuel cell with a platinum catalyst. PEMFC are generally the most economical type of fuel cells available and have the advantage of operating at low temperatures, but they have the disadvantage of being very sensitive to carbon monoxide and carbon dioxide contained within the fuel line.

1.2 Basic Governing Equations for a PEMFC

Now attention is directed to the specific PEMFC fuel that is being used in the experiments and how it works. The PEMFC has both a cathode and anode catalyst made of platinum suspended within a carbon fiber matrix. The polymer electrolyte membrane is made of DuPont Nafion® NRE212. Nafion® NRE212 is a perfluorosulfonate ionomer that is specifically designed to allow only the protons of the hydrogen to pass through via diffusion; electrons cannot pass through this polymer. The whole membrane has a 5 cm^2 square active area. The amount of platinum contained in the

catalyst is 1 mg/cm^2 at 20% wt Pt/C. The gas flow channels are made of high purity graphite (which has both high electrical conductivity at 900 S/cm and high thermal conductivity at 117 W/{m*K}). Gold current collector plates are mounted on the outside of the graphite. Between the graphite and the membrane there are also two plastic gaskets that help to create an airtight seal around the membrane. These gaskets also provide an additional electrical barrier between the cathode and the anode (see Figure 2 and 3). The whole setup is held together with plastic encased screws, which are tightened until the system is airtight.

Figure 2: Picture of Actual PEMFC

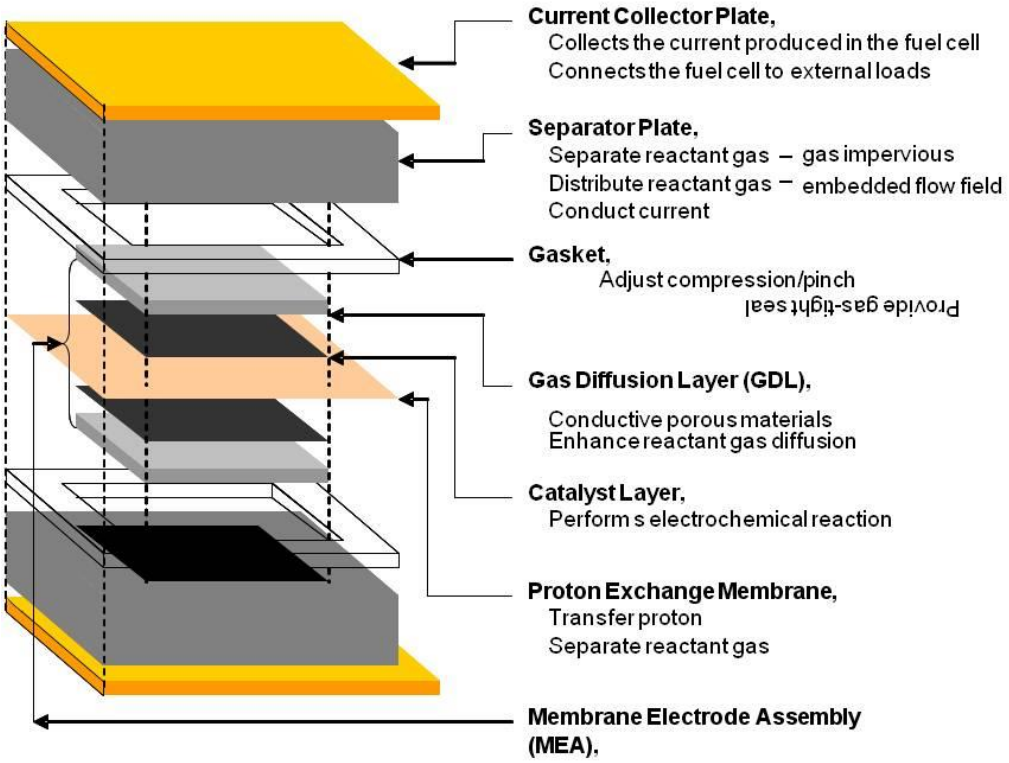

Figure 3: Manufacturer's PEMFC Schematic [29]

The fuel cell sits on a non-conductive stone pedestal. The gold plates have leads that allow devices to be connected in order to measure the electrical power being generated or to use the electrical power. This connection between the gold plates is required because the electrons need to flow from the anode to the cathode side. To use a familiar analogy, the anode side can be thought of as the negative side of a battery and the cathode side the positive. A device has to be to be connected to both sides to allow the electrons to flow from negative to positive. If a connection is not made, the gases will simply pass through the fuel cell unaffected and unused because the electrons are not able to flow.

As already described, the anode is where the hydrogen enters the fuel cell and is split by the platinum catalyst and only the protons from the hydrogen atoms are able to pass through the Nafion® NRE212. The electrons that were associated with the hydrogen molecules are only able to flow into the graphite and eventually into the gold, as both the Nafion® and plastic gaskets prevent any chance of a different path. The chemical equation associated with the anode side is [3]:

$$H_2 \rightarrow 2H^+ + 2e^- \quad (1)$$

The cathode side is where air enters the system. The oxygen molecules in the air are also split by the platinum catalyst. The protons from the split hydrogen and the free electrons available from the anode side combine with the split oxygen from this reaction to form water. The chemical equation associated with the cathode side is [3]:

$$1/2\ O_2 + 2H^+ + 2e^- \rightarrow H_2O \quad (2)$$

The global chemical equation associated with the total process between all 3 layers (anode, electrolyte, and cathode) is [3]:

$$H_2 + 1/2\ O_2 \rightarrow H_2O + \text{heat} \quad (3)$$

If the materials within the PEMFC had no electrical resistance, the system would have a maximum possible open source voltage of 1.192 V at 70 °C operating temperature [3]. Under that assumption, all of the Gibbs free energy available in the system would be converted into electrical energy and the maximum theoretical efficiency that the fuel cell could achieve would be defined as [3]:

$$\eta = \Delta G / \Delta H = 230.03 \text{ kJ mol}^{-1} / 284.52 \text{ kJ mol}^{-1} \text{ (at 70 }^{\circ}\text{C)} = 80.84\% \qquad (4)$$

Due to the fact that the PEFMC is comprised of real materials which all have electrical resistance of some magnitude (although it has been minimized), neither the maximum possible open source voltage nor the maximum theoretical efficiency can actually be achieved. Although the system uses gold and graphite which both offer very high conductivity material properties, and the Nafion® is specifically designed to offer very little resistance to the protons being diffused through it, these power losses due to resistance accumulate and result in a maximum expected possible open system voltage of approximately 0.93 V (per the manufacturer).

Similarly, temperature losses occur in the system because much of the heat used to bring the PEMFC to operational temperature is wasted by heating up the air surrounding the PEMFC (wasted to ambient). There is still debate over whether the Carnot efficiency is valid when applied to fuel cells. One of the major resources for this paper argues that it is not valid because the fuel cell is not a heat engine but rather, a chemical convertor [3]. The issue with using the Carnot efficiency is what temperature is defined as the "cold" temperature, in this case the ambient. Carnot efficiency is defined as (assuming 70 °C PEMFC operating temperature and 25 °C ambient temperature):

$$\eta_{th} = 1 - T_C / T_H = 1 - 298.15 \text{ K (25 }^{\circ}\text{C)} / 343.15 \text{ K (70 }^{\circ}\text{C)} = 13.11\% \qquad (5)$$

The Carnot efficiency is dramatically less than the theoretical maximum efficiency, which is the source of the debate. Fortunately, with regards to the setup being used for these experiments and what is being examined here, efficiency is not relevant because only the effects of different molecules added to the anode side are being analyzed. Additives will reduce efficiency, but this loss can more directly be measured by comparing the total maximum power output from the PEMFC with and without the additives. Power is defined as:

$$P = V * I \tag{6}$$

where power is P, voltage is V, and current is I. The current is the rate of electron flow being drawn to power a device. The more current extracted from the system, the more the voltage will decrease. For any given PEMFC, there is a voltage/current curve. Following this curve eventually the system will yield zero voltage, at which point the current magnitude is referred to as "short circuit current." The beginning of the voltage/current curve is the aforementioned open source voltage.

The maximum power that the PEMFC can output for a given set of input factors falls somewhere along the curve between the short circuit current and the open source voltage. The shape and length of the curve can be altered by varying any of three input factors to increase the amount of power the PEMFC is capable of generating. These factors are: pressure, temperature, and relative humidity. Each of these factors alters the nominal value of the short circuit current and the shape of the graph between the open

source voltage (no current) and the short circuit current (no voltage). Typically only two of the three factors are altered, with temperature always being one of the two altered because it is the easiest to control. In the present case, temperature and relative humidity will be attered.

1.3 Issues Currently Affecting PEMFCs

Given all of the advantages of PEMFCs, why are they not in widespread use today? There are five major issues hindering mass adoption. Some issues are merely functional, such as a lack of a mass delivery system. For example, there are a very limited number of hydrogen filling stations where one could refuel a fuel cell car (analogous to a gas station). This is a simple supply and demand issue that is not related to the present research. Other issues currently being researched include more efficient storage methods for hydrogen, creation of clean hydrogen sources, effective water mitigation techniques for high efficiency fuel cells, and reduction and quantification of catalyst poisoning.

The hydrogen storage method currently in use commercially involves storing hydrogen in liquid form or as a pressurized gas. Large amounts of energy are required to get the hydrogen into the desired states and it is unstable and dangerous as a pressurized gas (although the gaseous state requires less energy to compress than the more stable liquid state). Current research in the area of hydrogen storage is focused on methods of addressing both the energy and safety issues. One of the most appealing

concepts under investigation is storing the hydrogen in a porous media at ambient conditions [4].

The primary commercial sources of hydrogen are currently steam reformation of fossil fuels and electrolysis of water (i.e., the exact reverse of what a fuel cell does). Of these two, the steam reformation method is more widely used. Although this process creates a large quantity of hydrogen-rich fuel source, the process also creates carbon monoxide and carbon dioxide and traditionally uses fossil fuel. Current research is investigating methods of replacing the fossil fuel with a renewable hydrocarbon such as methanol or ethanol [5,6,7,8]. While using these biofuels still produces carbon monoxide and carbon dioxide, it does not consume our limited supply of fossil fuel resources and therefore can yield an endless supply of hydrogen rich fuel.

Water mitigation is an issue seen on the cathode side of highly efficient fuel cells or stacks of fuel cells. In highly efficient fuel cells or stacks of fuel cells, the water production on the cathode side can be so large that it actually causes the membrane to be flooded. Flooding occurs when the membrane is covered by water and the platinum is thus prevented from reacting with the desired gas. The water also poses a freeze/thaw issue in colder climates, where physical damage to the fuel cell(s) could result from expansion and contraction of the water. Current research is investigating altering the design of the cathode side, for example by adding a channel in order to provide another

means for water to exit the system or by setting up humidification cycles to turn on and off the relative humidity being added to the lines [9,10,11,12].

The final issue, catalyst poisoning, is what is being investigated here. This issue arises when additives are contained within the fuel being added to the anode side of the PEMFC. These additives are usually byproducts of the steam reformation process. As previously discussed, these byproducts are carbon monoxide and carbon dioxide. Carbon monoxide is known to be the more damaging of the two as these molecules strongly bind to the platinum catalyst, which results in the carbon monoxide being permanently adsorbed to the catalyst. This agglutination of the two molecules effectively makes the platinum site inactive such that it will no longer split hydrogen [13,14,15]. Within any PEMFC there are a finite number of platinum sites available. As the number of available sites declines due to poisoning, so does the overall effectiveness of the fuel cell. Fewer available platinum sites result in a reduced chemical reaction rate, and therefore reduced electrical energy generation. The carbon monoxide poisoning is described by the following chemical equations [13]:

$$H_2 + 2\,Pt \rightarrow 2\,Pt\text{-}H_{ads} \quad (7)$$

$$CO + Pt \rightarrow Pt\text{-}CO_{ads} \quad (8)$$

$$2\,CO + 2\,Pt\text{-}H_{ads} \rightarrow 2\,Pt\text{-}CO_{ads} + H_2 \quad (9)$$

The other poisoning agent investigated was carbon dioxide. Currently accepted research indicates that the platinum catalyst *can* also split carbon dioxide, forming a

carbon monoxide molecule and returning us to the carbon monoxide issue previously discussed [13,16,17,18,19]. However, there is significant debate over whether the splitting actually *does* occur and if it does occur, whether the effects are significant enough to be detected [13,16,17,18,19]. The carbon dioxide splitting has been shown to occur only under certain very specific conditions, whereas the carbon monoxide reaction occurs under any conditions. The chemical equation for the carbon dioxide effect is [13]:

$$CO_2 + 2\ Pt\text{-}H_{ads} \rightarrow \quad Pt\text{-}CO_{ads} + H_2O + Pt \qquad (10)$$

In both cases, the term Pt- CO_{ads} appears. This term represents a platinum site with adsorbed carbon monoxide, rendering it inactive. This effect is irreversible. Although cleaning methods exist to restore some of the platinum sites, even those methods do not have a 100% recovery rate. Therefore, once a platinum site has been poisoned by carbon monoxide the overall power level and efficiency of the fuel cell is permanently diminished.

Different approaches are under investigation to address this catalyst poisoning issue. One such approach is to change the catalyst by adding an additional metal more attractive to carbon monoxide. One metal in use currently in use for this purpose is ruthenium. This approach merely increases the carbon monoxide tolerance of the catalyst rather than immunizing the catalyst, similar to using a rust coat on an I-beam. The beam will still rust, albeit at a significantly reduced rate. This study used a different

approach whereby the carbon monoxide was cleaned out of the fuel before the fuel was added to the PEMFC and only the carbon dioxide and hydrogen were present.

1.4 Project Goals and Milestones

One of the main goals of the Thermodynamics and Sustainable Energy Laboratory is to create a Hybrid Solar System (HSS) [20]. The HSS is to consist of four main processes: solar steam reformation, fuel cleaning via a preferential oxidation reactor (PROX), hydrogen storage, and the PEMFC. This system will proceed in the following way when all four components are connected (refer to Figure 4): methanol will be added to the steam reformer, which will be heated only by sunlight. The solar steam reformer will convert the methanol into a hydrogen rich fuel that also contains carbon monoxide and carbon dioxide (75% H_2, 24% CO_2, 1% CO). The resulting hydrogen rich fuel will be input into the PROX, which will convert it into a mixture of hydrogen and carbon dioxide (75% H_2 and 25% CO_2) containing only trace amounts of carbon monoxide (< 10 ppm, as any higher concentration would poison the platinum catalyst). The cleaned fuel will then be input into the PEMFC where it is converted into electrical energy. Any excess fuel remaining will be stored for nighttime use, because the reformer requires sunlight to operate. Excess heat from the solar steam reformer will be used to heat other components of the system such as the boiler for the fuel cell, the fuel cell itself, and the PROX.

The key goal of this research is to determine whether, given the debate over the effects of carbon dioxide on the membrane [13,16,17,18,19], it is feasible to run this PEMFC on the expected gas mixture from the solar steam reformer after it is cleaned by the PROX (75% H_2 and 25% CO_2) with no significant power loss and no long-term damage to the membrane. If this can be achieved, it will validate the overall concept of the HSS. To accomplish this key goal, several concrete milestones were defined: design, construct, and operate a stable setup; verify effects of relative humidity and temperature; find the optimal operation point; add carbon dioxide into the anode fuel source; and add the PROX (fed by the exact gas mixture expected from the solar steam reformer) into the setup.

The first milestone was to design and build a PEMFC setup that used relative humidity and temperature as the variable inputs. This setup needed to demonstrate stability over time. The next milestone was to verify the effects of varying relative humidity and temperature on fuel cell performance. Once those effects had been quantified, an optimal operating point was established. After these three initial milestones were achieved, a baseline power level using pure hydrogen was established.

Carbon dioxide was then introduced into the hydrogen stream at varying levels and the resulting power levels were compared to the baseline. Once the carbon dioxide data was analyzed, a determination was made (based on the change in power levels) as to whether the PROX should be attempted. If the determination was made to proceed

with PROX, it was added to the setup and fed by the exact gas mixture expected from the solar steam reformer. Power levels were again compared to the baseline to determine the feasibility of the HSS.

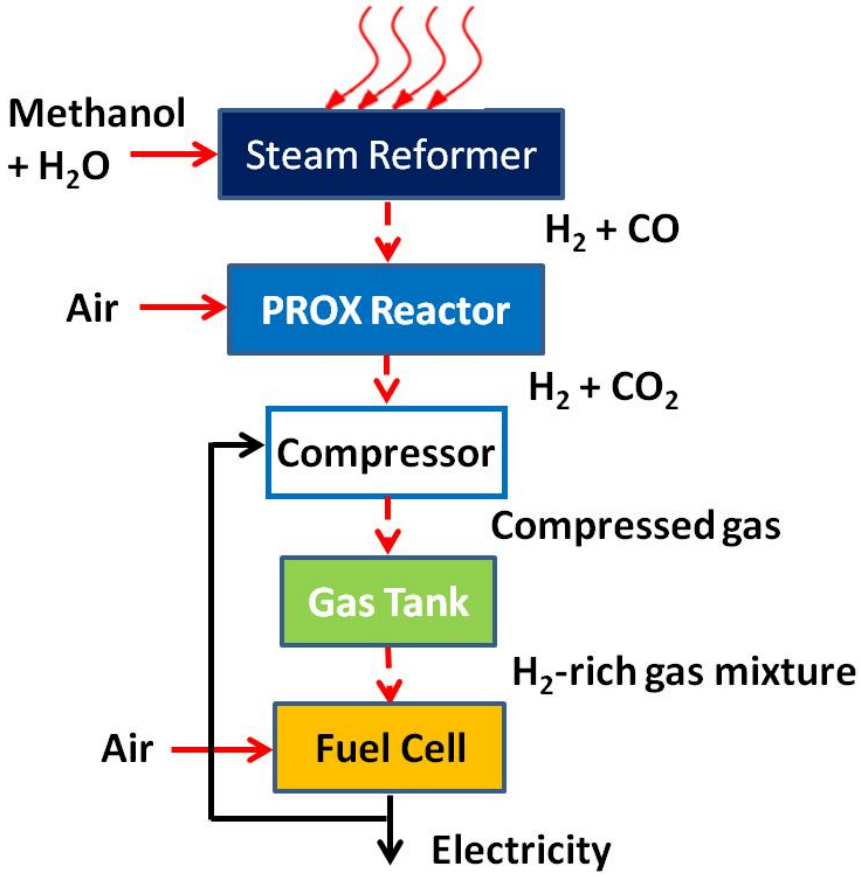

Figure 4: HSS Flowchart [20]

2. Experimental Setup / Procedure

Attention is now turned to the setup design and rationale. At the most basic conceptual level, the setup needed to contain: inlets to deliver gases; a boiler to add humidity into the gases; a PEMFC to convert the gases into electrical power; a load (in this case a measuring device, the Keithley Model 2440 SourceMeter); and gas outlets. The setup also needed to have the ability to vary the relative humidity and fuel cell temperature. Additionally, gas flow rates into the setup needed to be controlled. All of the gases used in the setup followed the ideal gas law model (especially when calculating mixtures) [21]:

$$p * v = n * R * T \tag{11}$$

where p is pressure, v is volume, n is quantity in moles, R is the ideal gas constant, and T is temperature. This is critical because the flow rate of the hydrogen gas can dramatically affect power output. Unless otherwise noted, all tests held the hydrogen rate at 5 ccm (or 5 ml/min) and the air rate at 50 ccm (or 50 ml/min) and tests had a duration of 3 hours. In our setup, pressure and temperature were constant. Therefore, when looking at the gas mixtures the ideal gas law model can be simplified to [21]:

$$X_{H2} = n_{H2} / (n_{H2} + n_{CO2}) = V_{H2} / (V_{H2} + V_{CO2}) \tag{12}$$

where X_{H2} is the percentage of hydrogen within the mixture. Rather than looking at volume and moles as a static number such as a liter or gallon, n_{H2} and n_{CO2} represent the rate of moles of the substances being added and removed from the system. Similarly,

V_{H2} and V_{CO2} are the volumetric flow rates of the substances being added and removed from the system. These rates do not change over time at the inlet. Table 1 below shows of all the flow rates that were used during the experiments.

Table 1: Flow Rates

Gas Mixture	H_2 (ccm)	Air (ccm)	CO_2 (ccm)
100% H_2 0% CO_2	5.00	50.00	0.00
90% H_2 10% CO_2	5.00	50.00	0.56
80% H_2 20% CO_2	5.00	50.00	1.25
75% H_2 25% CO_2	5.00	50.00	1.67
70% H_2 30% CO_2	5.00	50.00	2.14

2.1 Relative Humidity

Relative humidity is the measure of the amount of water vapor contained within the gas being fed into the PEMFC. Higher relative humidity increases the effectiveness of the electrolyte. The main function of the electrolyte is to be a high protonic conductivity material [3]. For this experiment, the electrolyte material was a perfluorosulfonate ionomer called Nafion® NRE212. As previously discussed, the function of the electrolyte is to allow protons from the split hydrogen to diffuse through it while blocking electrons. The relative humidity increases the electrolyte's protonic conductivity. Therefore the higher the relative humidity, the more efficiently the hydrogen protons will diffuse through the electrolyte [3,23,24]. The faster the hydrogen diffuses through the electrolyte, the faster the protons will be available on the cathode side to form water and complete the cycle. Relative humidity is dependent on saturation

vapor pressure and temperature. In this case, the desired relative humidity level and atmospheric pressure set the saturation vapor pressure. Therefore, relative humidity becomes only a function of temperature. Relative humidity is defined using the Antione Vapor Pressure Correlation as [22]:

$$\ln (p_{vp}) = A - B / (T+C) \quad (13)$$

$$RH = p_{vp} / p_{atm} \quad (14)$$

where RH is relative humidity, p_{atm} is atmospheric pressure (760 mmHg), p_{vp} is saturation vapor pressure, T is temperature, and A/B/C are constants of the medium (in this case, water). These constants are: A = 8.07131, B = 1730.63, and C= 233.426 for water between 0 ˚C and 100 ˚C. Table 2 below displays all relative humidity values used in the experiments and the resulting isothermal water bath temperatures required to achieve these relative humidities.

Table 2: Relative Humidity and Required Temperature

RH (%)	p_{vp} (mmHg)	T (˚C)
5%	38.0	33.2
7%	53.2	39.3
10%	76.0	46.1
15%	114.0	54.3
20%	152.0	60.4
25%	190.0	65.3
30%	228.0	69.5
35%	266.0	73.1
40%	304.0	76.3

As shown in Table 2 above, the temperature of the gas directly controls relative humidity. These relative humidity levels have been experimentally tested and confirmed by analyzing the gas flow to see if it they have achieved full saturation using a hydrometer (see Section 2.4 for further details). At a given temperature, the setup adds as much water into the gas as the gas can possibly hold. This is achieved by running the desired gases through boilers that are contained within an isothermal water bath set at the desired temperature for chosen relative humidity level (the anode and cathode side gases have separate boilers to prevent any mixing prior to reaching the PEMFC). The humidified gas is then delivered to the PEMFC and processed.

The anode side and cathode side do not require equivalent relative humidity levels, but the present setup is limited by the amount of isothermal water baths available to heat the boilers which control relative humidity. Usually, the anode side needs more humidification than the cathode side because the water from the reaction is created on the cathode side of the PEMFC. When both sides have the same relative humidity level, the excess water on the cathode side could cause flooding and lead to power degradation over time because the water created by the PEMFC has nowhere to exit the system other than by being pushed by the gas flow. Ideally, this water that has been created would be carried by the gas (absorbed within it) out of the system. If the temperature in the conveyance system drops below the set point of the corresponding relative humidity setting, water will condense out of the gas flow because the threshold

for the maximum amount of water for the lower temperature has been exceeded and the gas flow would adjust to a lower relative humidity level (refer to Table 2 above, lower temperatures cause lower relative humidity levels, thus excess water is removed via condensation). If the temperature in the conveyance system rises above the set point temperature, the gas has an increased holding capacity and can absorb more water if needed. Current research investigating the relative humidity aspect of fuel cells deals either with high temperature fuel cells where the membranes are dehydrated due to extremely high operating temperatures and are thus losing protonic conductivity in the electrolyte [23], or with high efficiency fuel cell stacks where the amount of water creation within the system affects the timing of the humidification by turning on and off the gas humidification as needed (mainly on the cathode side) [24].

2.2 Operating Temperature

Operating temperature affects the PEMFC in five major ways: 1) voltage losses within the materials; 2) PEMFC's overall maximum theoretical efficiency; 3) level of protonic conductivity; 4) quantity of chemical reactions; and 5) rate of diffusion [3,25,26,27]. PEMFCs have the ability to run at temperatures ranging from 0 ˚C to 120 ˚C. While a PEMFC can operate at freezing temperatures, generally the power output will be dramatically lower than at higher temperatures [3,25]. Ideally, PEMFCs would run at an operating temperature of 120 ˚C to achieve maximum theoretical efficiency. Unfortunately, PEMFCs usually have a maximum operating temperature of 100 ˚C,

limited by the heat tolerance of the polymer electrolyte and the boiling point of water. SOFC are normally used for operating temperatures exceeding 100 ˚C [13]. The most efficient temperature range for a PEMFC is between 60 ˚C and 80 ˚C [3,25]. In large fuel cell stacks, enough heat is generated by chemical reactions to maintain the desired operating temperature using only a startup aid. In single fuel cell systems, such as the present PEMFC, external heaters are used to both reach and maintain desired operating temperature because the amount of heat generated by chemical reactions is negligible compared to the large size of the experimental setup.

Voltage losses in the PEMFC's materials (gold and graphite) decrease as the electrical conductivity of the material increases [3,25]. The operating temperature increases the electrical conductivity of the materials by improving the ability of those materials to transfer the free electrons (i.e. decreasing resistance). The lower the overall resistance in the system, the more likely it is that the actual efficiency of the PEMFC will approach maximum theoretical efficiency.

One drawback to increased operating temperatures is that as the operating temperature rises, the PEMFC's overall maximum theoretical efficiency decreases. This phenomenon is due to a decrease in the amount of Gibbs free energy [3]. However, this decrease in maximum theoretical efficiency is often ignored because maximum theoretical efficiency is merely a measure of what the fuel cell could *possibly* produce

rather than what it will *actually* produce. The other benefits of the rise in operating temperatures completely offset this negligible effect.

Another drawback to increased operating temperatures is that the protonic conductivity of the electrolyte decreases [3,25,26]. The decrease in the protonic conductivity is an increase to the system's overall resistance, because the electrolyte material has increased resistance to diffusion of the protons. This decrease in the protonic conductivity is caused by dehydration of the membrane. As previously discussed, water is required in order to facilitate the reaction, especially on the anode side. This drawback can be overcome by increasing the relative humidity of the gas in order to offset the increased operating temperature that is causing the dehydration of the membrane. Therefore, if you increase operating temperature you would need to increase the relative humidity. Because the PEMFC generates power by converting chemical energy into electrical energy, if you could increase the quantity of chemical reactions you could increase the power. If heat is added to any chemical reaction the reaction will speed up, thus creating more reactions in a given time span.

While rising operating temperatures decrease the protonic conductivity of the electrolyte material, the actual mass transport phenomenon of diffusion increases with temperature [26,27]. Because the PEMFC depends on diffusing one material into another (in this case a hydrogen proton through the electrolyte), heating it up will decrease the time needed to complete this process.

2.3 Setup #1

This setup was inherited from previous experiments. A hot plate was used to heat a large vessel that contained the isothermal water bath, in which two 50 mL boiler vials were set up to control the relative humidity of both gases. The lines leading from the boilers were wrapped in a single thin Omega heat wire in an attempt to maintain the gas at temperature until it reached the PEMFC (see Figure 5).

The PEMFC is a single cell (ElectroChem PEMFC) that contains a 20% wt Pt/C at 1 mg/cm^2 membrane. The cell inputs the gas in a serpentine flow pattern onto a 5 cm^2 section of the membrane. This specific PEMFC remained unchanged throughout all experimental setups with the exception of membrane electrode assembly replacement (using an identical MEA), thus no further mention of its statistics is made. This PEMFC has an external heater attached to both sides of the gold plates pre-installed by the manufacturer. All heat to the Omega heat wire and fuel cell heaters is controlled by external electrical thermocouples that turn on/off the power based on a set temperature point governed by an Omega temperature controller. The hot plate controlling the isothermal water bath was heated by turning the hot plate on/off based on a digital thermometer reading and ice was used if rapid cooling was needed.

When examining a single time interval, the current / voltage curves produced appeared typical. This was the goal of previous experiments. However as shown in Figure 6, problems with the setup became apparent when maximum power was plotted

across multiple time intervals under identical conditions. Huge instabilities in the power curve were observed, which were unacceptable for the purposes of the present experiment. For this experiment, the setup needs to generate a constant power curve so that when the gas mixture is varied the resulting curves can be quantified and qualified. To generate consistent data suitable for use in comparing power curves, the setup needed to be stabilized in order to minimize fluctuation of the maximum power during the course of a 3-hour run. Therefore, modifications to the setup were needed.

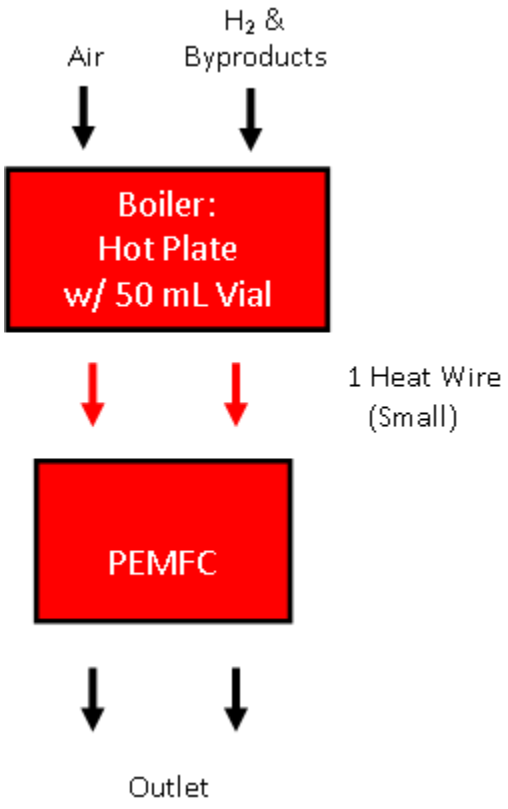

Figure 5: Setup #1 Flowchart

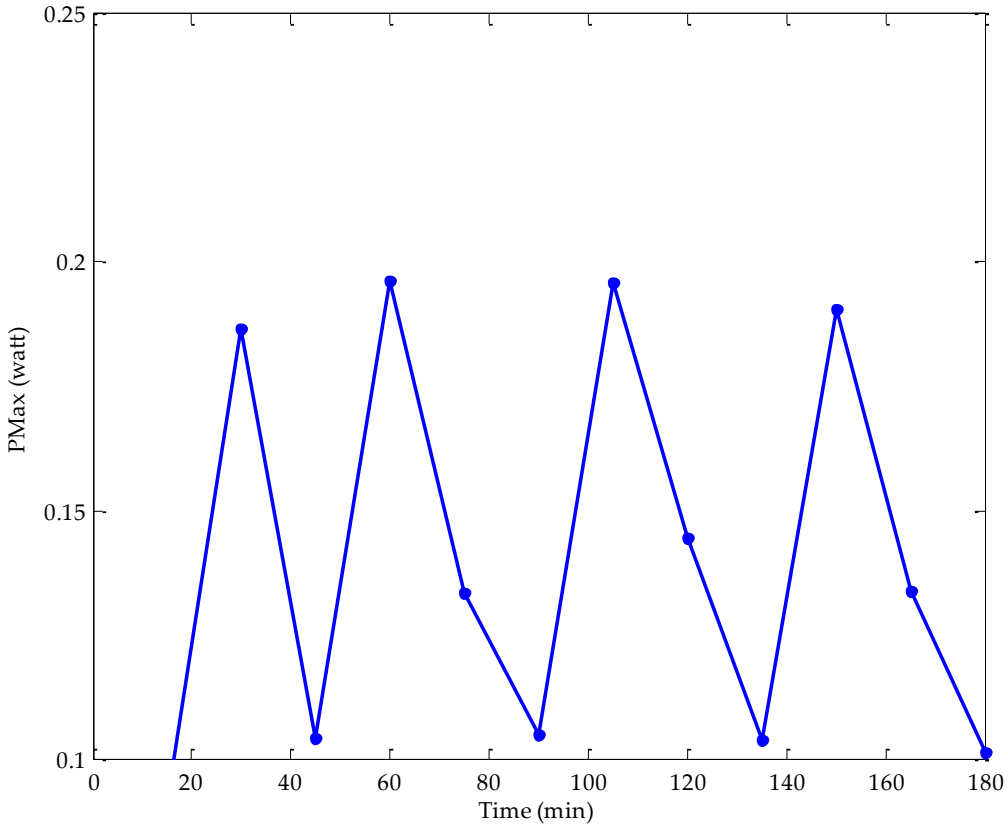

Figure 6: Setup #1 Power Curve Analysis Across Multiple Time Intervals

2.4 Setup #2

The previous setup was analyzed for defects. The issues that could be visually identified were: evidence of condensation in the lines carrying the humidified gases; an excessive amount of mechanical connections; and an inability to maintain a specific relative humidity.

The easiest change to make was to remove excess mechanical connections. The original setup had several fittings installed solely to provide easy connection of the PEMFC. These extra fittings added resistance (analogous to adding a resistor in an

electric circuit) into the flow lines, causing pressure drops [1]. The overall system was reviewed and the total amount of mechanical connections and pipe lengths were reduced to the bare essentials needed to operate the system (see Figure 7). This revision to the system was intended to also mitigate the condensation issues. The theory was that if the pressure drops in the system were reduced then the ability of the system to remain at temperature would be improved.

Next the system was tested for its ability to achieve a specific relative humidity. To test the relative humidity of the gases each line was allowed to run through the isothermal water bath and boiler and into a separate empty vial at the same temperature as the isothermal water bath and the output was measured with a hydrometer. The relative humidity was found to be below expectations; therefore, modifications to the boiler setup were needed.

First, the size of the boiler vials was increased from 50 mL to 125 mL. The purpose of this was to allow the gas more time to absorb the water. Next, the hot plate (± 10 ˚C) was replaced with a Buchi Heating Bath Model B-491 (± 1 ˚C). The second modification increased the temperature stability of the isothermal water bath. As previously discussed in Section 2.1, temperature stability is vital in order to achieve a desired relative humidity. At higher relative humidities (above 20%) if the temperature of the isothermal water bath varies by even ± 1 ˚C the relative humidity is altered by ± 1%.

As shown in Figure 8, the modifications were beginning to have the desired effect of stabilizing the power curve. The power curve was significantly more stable than its predecessor, although it did still show some signs of instability. Therefore, further modifications were needed.

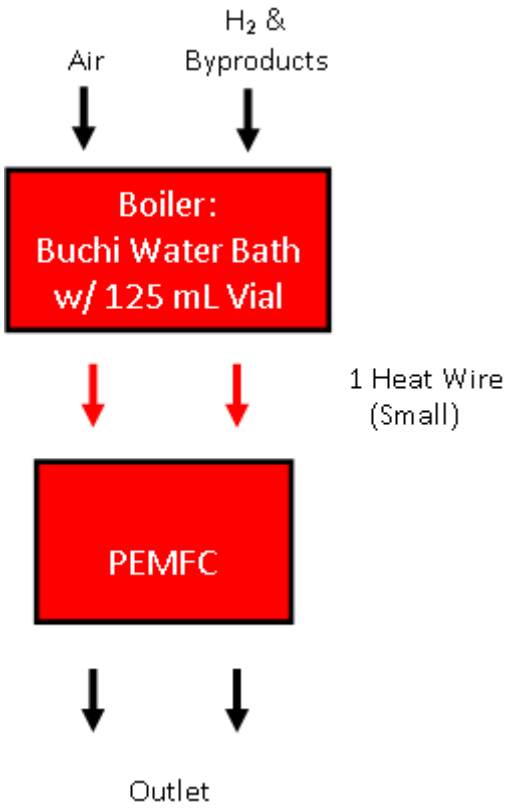

Figure 7: Setup #2 Flowchart

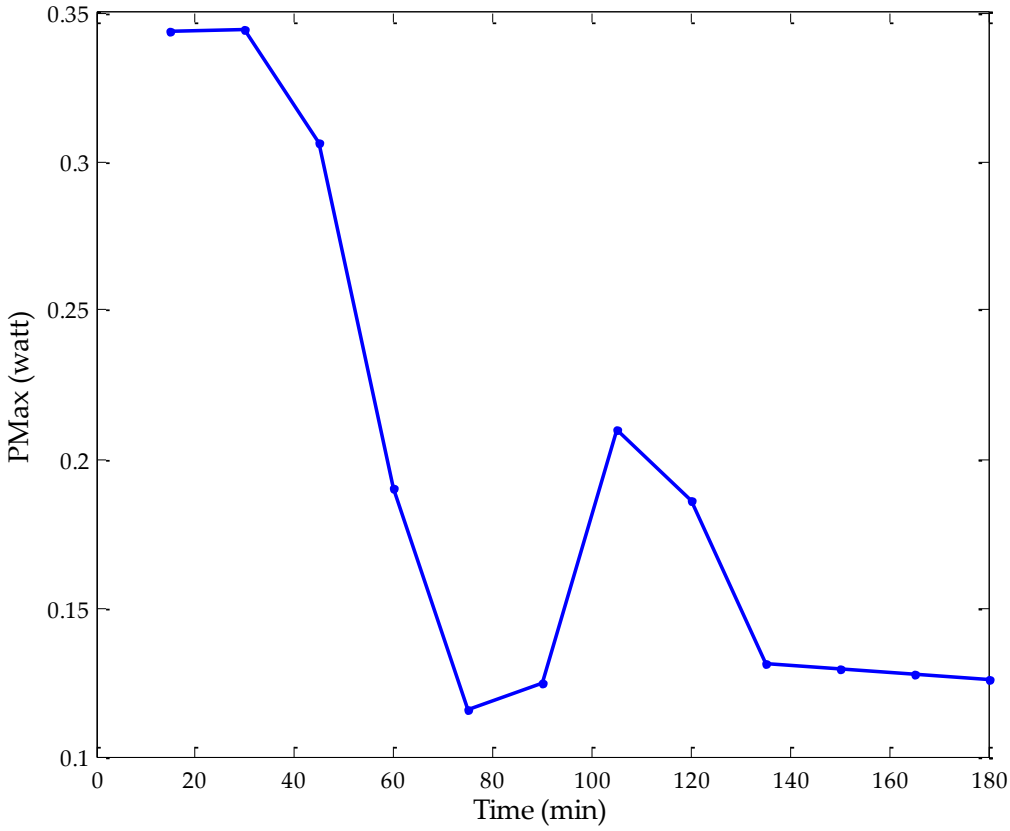

Figure 8: Setup #2 Power Curve Analysis Across Multiple Time Intervals

2.5 Setup #3

The setup was again analyzed for defects over the course of several runs. There continued to be evidence of condensation in the conveyance lines carrying the humidified gases (although less condensation than in Setup #2) and startup issues were observed due to a water droplet.

To fix the condensation issues the setup needed to be modified in three different ways: the boiler had to be physically modified, more heat had to be provided to the conveyance lines, and a condenser had to be added before the gas outlet.

First, the boiler system had to be modified in order to reduce the amount of heat loss in the gases during the transfer from the isothermal water bath to the heated conveyance lines (refer to Section 2.7 for in-depth description of the modification). The original design allowed some of the water to condense back into the boiler before the gases reached the heated conveyance lines, preventing it from reaching the relative humidity set point.

Next, additional heating wires had to be added to the system. The two conveyance lines directing the gases to the PEMFC were modified to be heated individually through the addition of heat wires. Originally, the two conveyance lines were heated together, causing a great deal of heat loss. Similarly, a heat wire was added to the conveyance lines directing the gases from the PEMFC to the condenser. These heat wires were added to the system to ensure temperature control throughout the system, preventing condensation events within the conveyance lines (the reference to heat wires being "Small" or "Large," which is seen in all of the flowcharts, refers to the width of the heat rope being used which was either 1/8" or 1").

In the final modification, the condenser (referred to in the previous paragraph) was added between the PEMFC and the outlet in order to give the gases a chance to cool and release water before they exited the system. This reduced the chance of an outlet clog due to flooding.

Startup issues were correctly attributed to the initial water droplet that was seen in the outlet just after startup of the system. This water droplet formed due to the initial burst of gas into the boiler that led into the conveyance line when the gas was first released. The water plug immediately saturated the membrane of the PEMFC and caused an initial boost in performance before settling into to a steady state. A liquid trap was added to the system to capture the water droplet before it reached the PEMFC (see Figure 9). Unfortunately, the liquid trap worked too well. While it performed the task of catching any excess water droplets, it also led to a cold point in the system. The cold point caused the liquid trap to act like a condenser, reducing the relative humidity of the gas before it reached the PEMFC.

As shown in Figure 10, the modifications caused the power curve to become extremely linear. The liquid trap acting as a condenser prior to the PEMFC lowered the relative humidity of the gas, which eventually dehydrated the membrane. This dehydration caused the maximum power output over time to decline, resulting in a negative linear slope. Although achieving a negative linear slope was a significant improvement, the ideal power curve line should reflect a constant. Therefore, further modifications were needed.

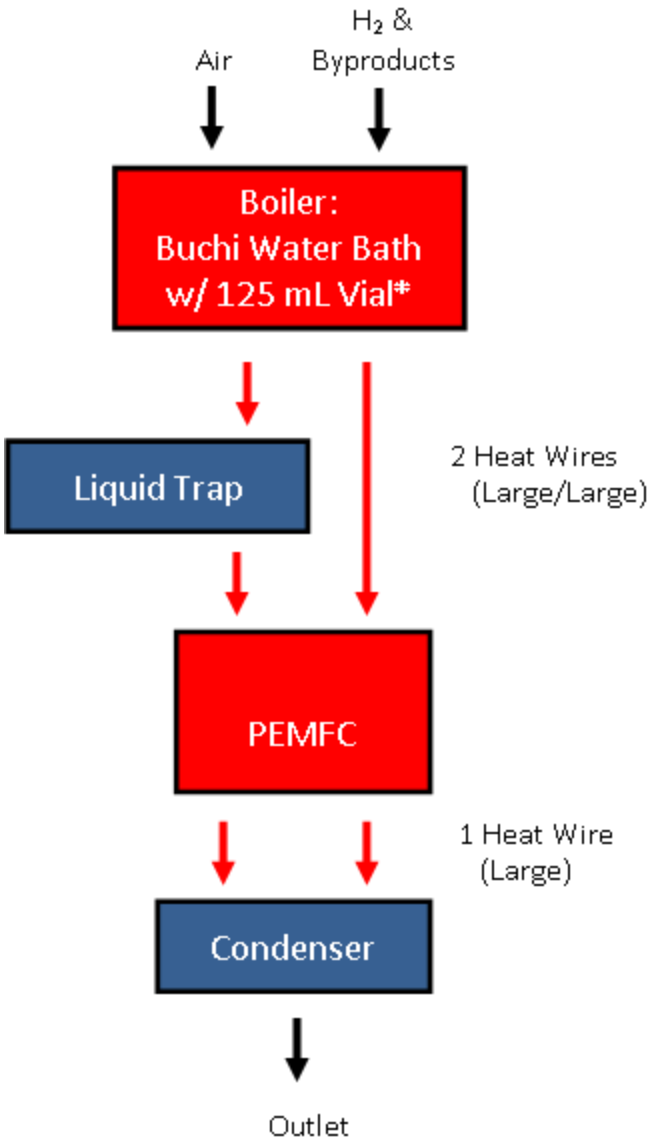

Figure 9: Setup #3 Flowchart

* the vial being used has been modified with the changes outlined in Section 2.7.

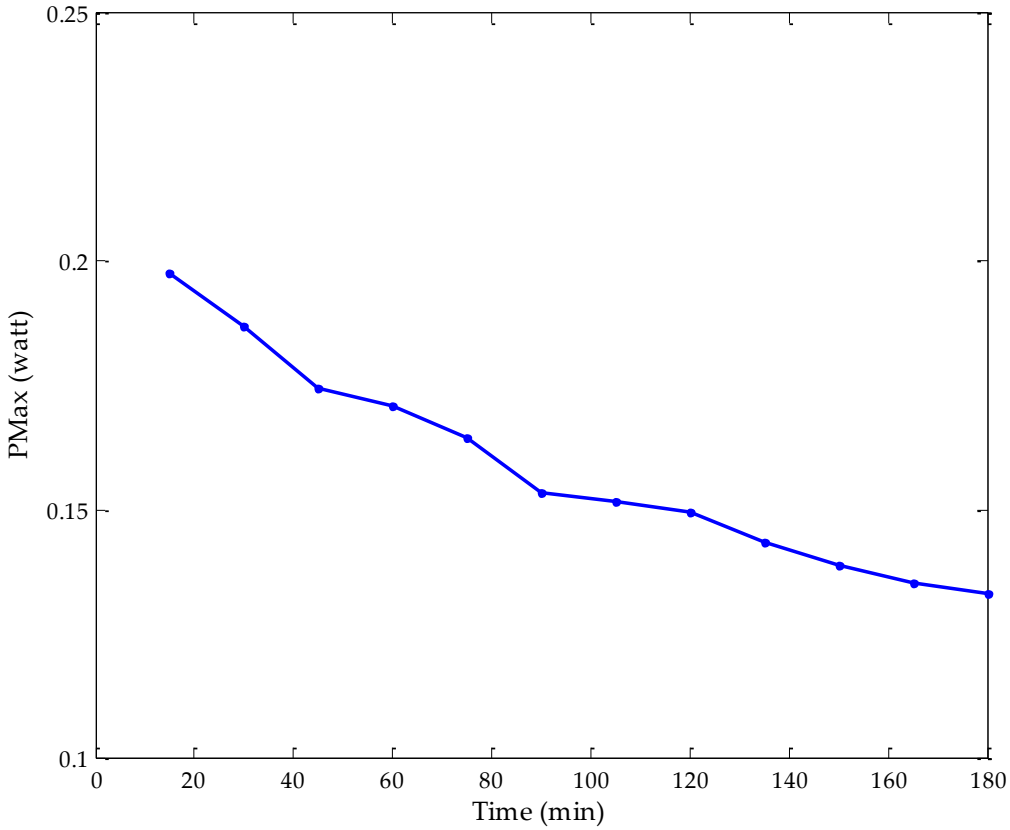

Figure 10: Setup #3 Power Curve Analysis Across Multiple Time Intervals

2.6 Setup #4

Although Setup #3 was a significant improvement over previous setups, it needed several modifications in order to address the remaining issue. The goal of the modifications was to prevent the water droplet discussed above from reaching the membrane of the PEMFC without causing condensation.

As previously mentioned, the liquid trap prevented the water droplet from reaching the membrane but was causing condensation and reducing the relative

humidity of the gas within the conveyance line prior to the PEMFC. The liquid trap added in Setup #3 was not an effective solution to the water droplet issue, so it was removed (see Figure 11). The modified boilers were again analyzed with respect to relative humidity using the same process discussed in Setup #2 (using the hydrometer to quantify results). This time, the amount of water in the boilers was varied across the tests. This allowed ideal water levels in the boiler to be set in order to achieve the desired relative humidity set points. Lower water levels within the vials provided enough protection so that the initial burst of gases did not cause the water within the boiler to splash high enough to gain access to the conveyance lines. Previously, the vials were filled almost full and the gap between the water levels and the conveyance line entrances was so short that the initial burst of gases caused the water to bubble into the conveyance lines and ultimately to be pushed by the gases into the PEMFC.

As shown in Figure 12, after making all of the aforementioned modifications the power curve became nearly ideal. The curve is almost constant with a very slight negative slope. This very slight negative slope can be attributed to the relative humidity settings used for the experiment. This is due to the fact that the gas on the cathode side was supplied with as much water as it could hold at the set point. Therefore, the water created by the PEMFC could not be absorbed into the gas and could only be physically pushed out of the system by the flow. This caused a flooding effect that slowly built up over time. To correct this, two different relative humidity settings for the gases supplied

to the PEMFC would be required. This would require using two isothermal water baths, and only one was available. Therefore, despite the slight negative slope to the power curve it was determined that this was the best setup for the experiments. The only further modification needed for a later experimental purpose was the addition of the PROX.

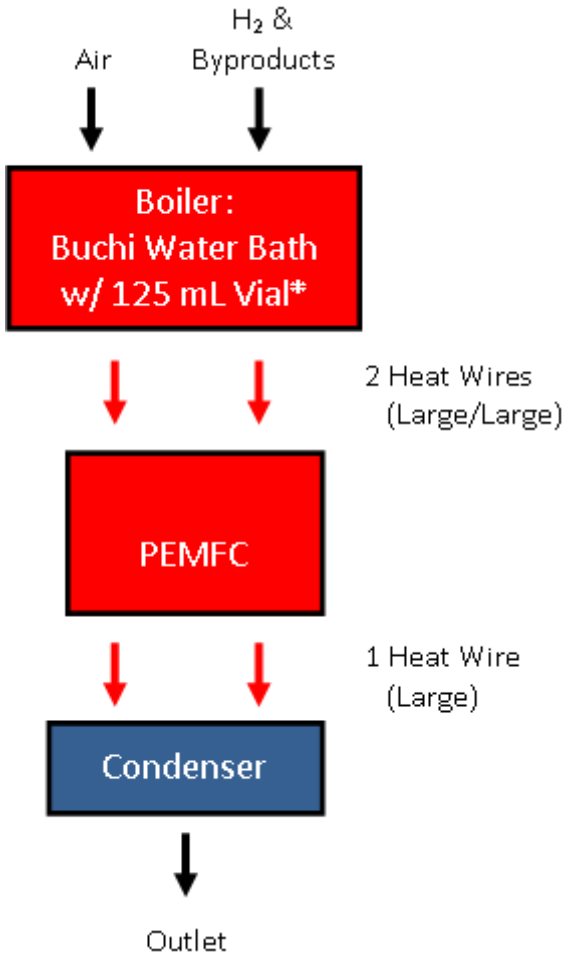

Figure 11: Setup #4 Flowchart

* the vial being used has been modified with the changes outlined in Section 2.7.

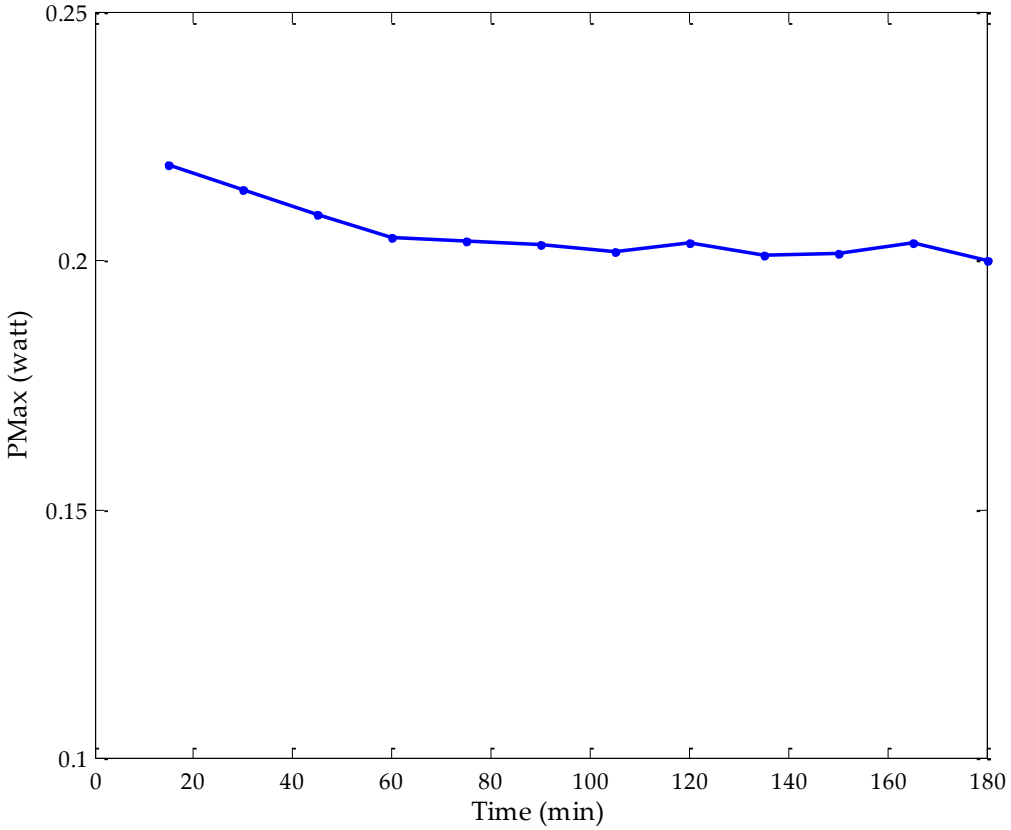

Figure 12: Setup #4 Power Curve Analysis Across Multiple Time Intervals

2.7 Boiler Modifications

The boiler modification discussed briefly in Setups #3 and #4 was the key to stabilizing the system over time. One of the analyses performed when determining the defects in Setup #2 was to create thermal profiles of all the major fittings and the boilers. The fittings into and out of the PEMFC were found to have slight heat losses associated with them. These small heat losses were addressed through modification of the wrapping technique of the heat wire.

It was also discovered that there were very large temperature drops during the transfer of the gases from the water within the boilers to the heated conveyance lines that lead to the PEMFC (see Figure 13). These temperature drops were attributed to the physical gap between the end of the isothermal water bath and the beginning of the heat wire. The purpose of the gap was to reduce the risk of the non-insulated heat wire touching the water and causing a shocking hazard. These temperature drops were located near the corks of the boilers and caused condensation prior to the gas flow entering the conveyance lines. This prevented the relative humidity set point from being achieved. Therefore, modifications to the boilers were needed in order to reduce this gap and thus reduce the heat losses.

Boxes were fitted over the top portion of the boilers (see Figure 14). The boxes were positioned in such a way that they would affect only the air gaps and corks within the boilers and leave the water contained within them unaffected, which is crucial because it controls the relative humidity. The walls of the boxes were sized to accommodate the evaporation of the isothermal water bath during experimental runs, preventing the water level of the isothermal water bath from falling below the bottom of the boxes. This permitted additional heating because the heat wire could be placed within the bottoms of the boxes, allowing the heating to continue all the way to the PEMFC. As a result, there was no longer a gap to facilitate heat loss because where the isothermal bath ended the heat wire began. Even the plastic material the box was made

of was heated by its contact with both heat sources (the isothermal water bath and the heat wire).

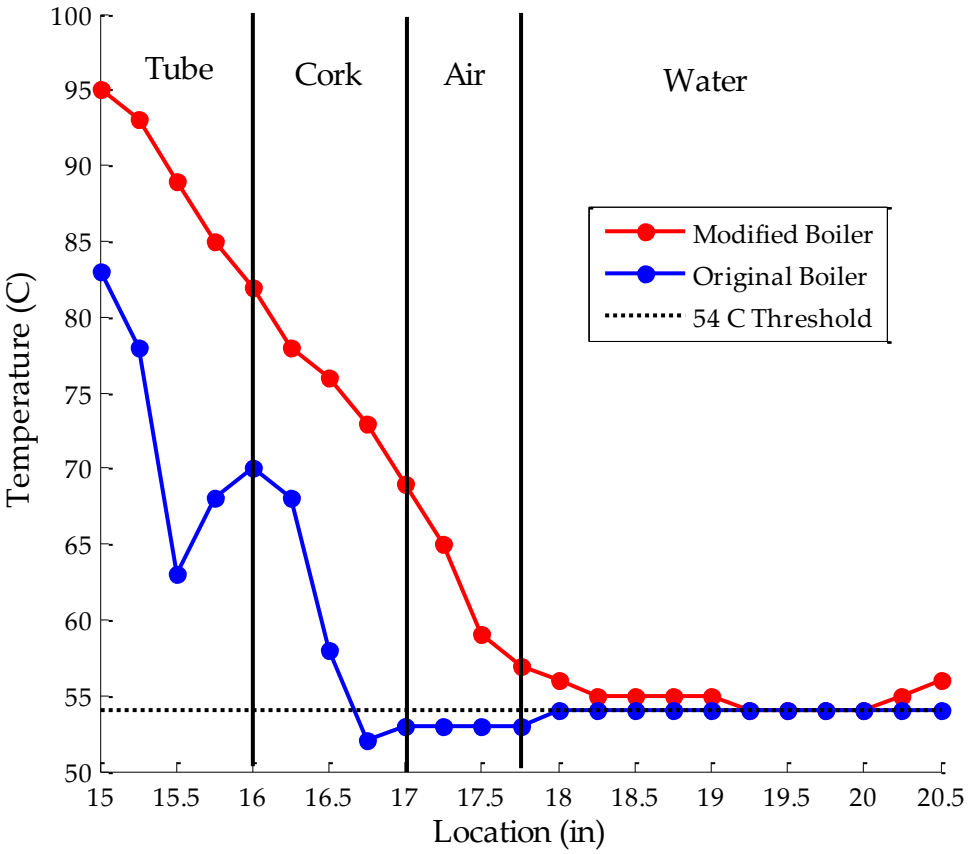

Figure 13: Boiler Temperature Profile Comparison

Figure 14: Picture of Actual Boiler

2.8 PROX

The purpose of the preferential oxidation (PROX) catalyst in the setup was to convert any carbon monoxide within the gas leading to the anode side into carbon dioxide, therefore removing the harmful molecules from the flow. The benefit of using a PROX catalyst is that can it can be tailored to affect only the carbon monoxide in the flow and to leave other molecules unaffected, preventing oxidation of the hydrogen back to water prior to the PEMFC. In the HSS (see Figure 4), methanol will be steam reformed via sunlight into a hydrogen rich source containing hydrogen, carbon dioxide, and carbon monoxide. This mixture will then be fed into the PROX and the carbon monoxide will be converted into carbon dioxide. The PROX will need to remove all traces of the carbon monoxide within the flow, because if even 10 ppm of carbon monoxide remains within the flow it will cause irreversible damage to the platinum

catalyst contained within the anode side of the PEMFC. The PROX catalyst used in this experiment consists of gold and iron oxide particles (Au/α - Fe_2O_3). The PROX oxidizes the carbon monoxide through the iron oxide particles that are surrounding the gold. The gold particles are used to catch the carbon monoxide and hold it until oxygen transferred from the iron oxide particles has completed the oxidation reaction. Once this reaction has taken place, the gold releases the newly formed carbon dioxide back into the gas flow. This oxidation process can be described with the chemical equation:

$$2\ CO + O_2 \rightarrow \ 2\ CO_2 \tag{15}$$

The particular PROX used in the present setup differs from a typical PROX catalyst, in that it is the inverse of the usual system. In the present PROX, the gold particles are the larger particles (~ 15-25 nm) and the iron oxide particles are the smaller particles (~ 5 nm). It has been documented that this inverse PROX catalyst achieved 100% conversion at experimental conditions [28]. For the purposes of the present setup, the PROX will need its own boiler and external heaters. The PROX must be heated to 80 $^{\circ}$C for the oxidation to achieve the desired 100% conversion rate of the carbon monoxide. This section is meant to be a brief overall description of the PROX and its setup as it relates to the present experiment. For further details and overview concerning the PROX, refer to the works of Shodiya [28].

2.9 Setup #5

In this setup (see Figure 15) the PROX system was added to Setup #4 (see Figure 11). This setup needed to accommodate two main features, which were that each system (PROX and PEMFC) could be run either independently or jointly and that the setup needed to be able to have a bypass leading to the gas chromatograph on the PROX side either before or during a run. The purpose of the setup was to test the overall concept of the HSS by inputting the expected gas mixture (75% H_2, 24% CO_2, 1% CO) from the solar collector into the PROX which would then clean that mixture (75% H_2 and 25% CO_2) and transfer the cleaned mixture into the boiler that would humidify it and finally convey it to the PEMFC [20]. The system had to allow for the output of the PROX to be tested via the gas chromatograph before allowing the flow to access the PEMFC in order to ensure that no carbon monoxide remained.

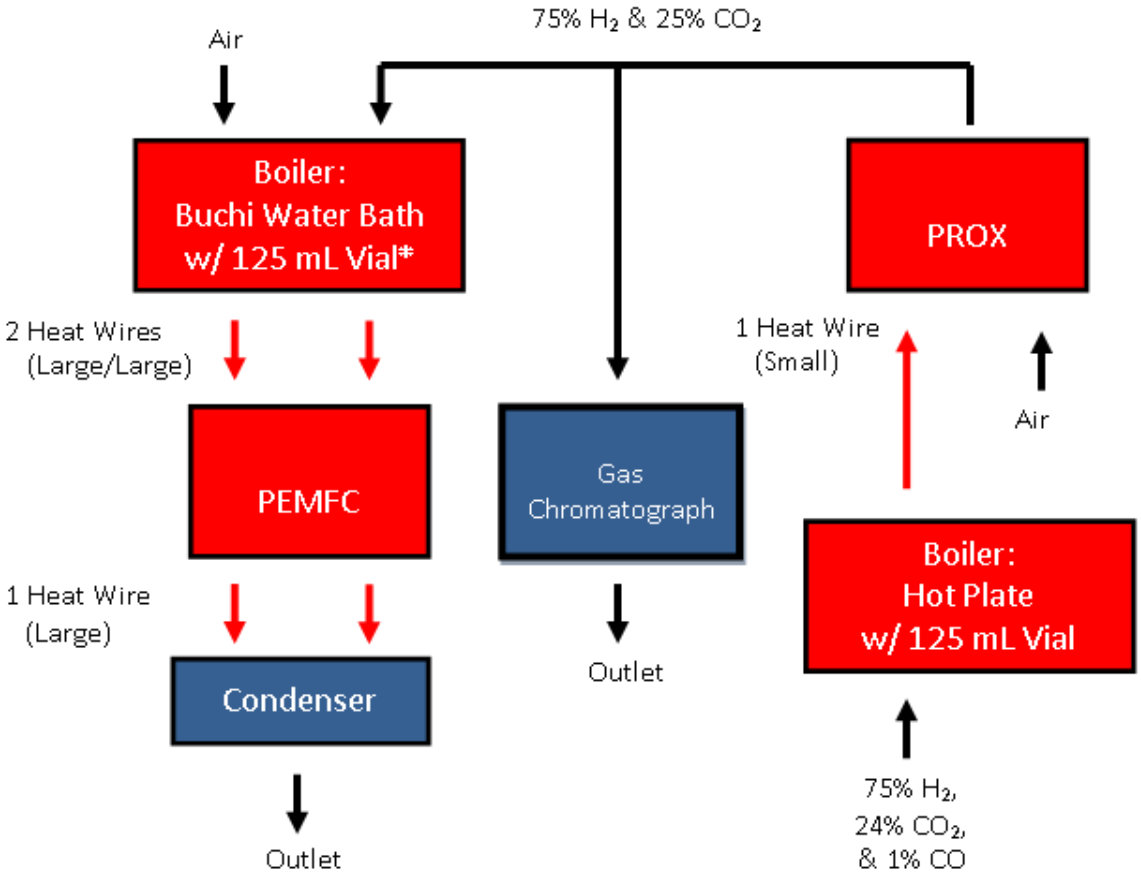

Figure 15: Setup #5 Flowchart

* the vial being used has been modified with the changes outlined in Section 2.7.

3. Results and Discussion

Setup #4 was used to test the effects of all of the following experiments with the exception of those in Section 3.5. Setup #5 was used to test this final experiment, which as previously stated used Setup #4 and simply added the PROX. Unless otherwise noted, all runs were performed over a 3-hour duration.

3.1 Effects of Operating Temperature on PEMFC Performance

As expected, as the operating temperature increased the power output from the PEMFC also increased. This trend continued until the operating temperature exceeded the relative humidity set point and the membrane began to dehydrate. This dehydration of the membrane decreased the protonic conductivity of the electrolyte, causing the power output to decrease. As shown in Figure 16, prior to this dehydration point an increase in operating temperature caused an increase in the short circuit current and caused the I / V (current versus voltage) curve to become more linear (instead of exponentially decaying). The tests shown in Figure 16 were run using flow rates of 5ccm hydrogen and 50 ccm air, with a fixed relative humidity of 25% and varying PEMFC operating temperatures.

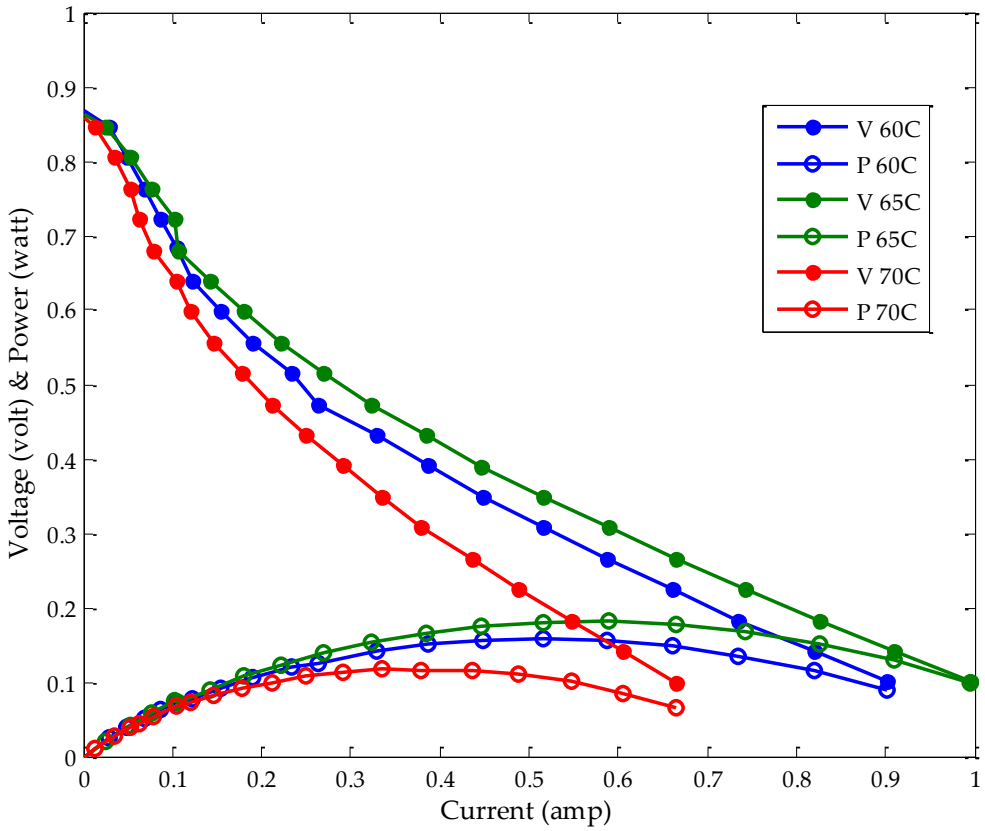

Figure 16: Effects of PEMFC Operating Temperature

3.2 Effects of Relative Humidity on PEMFC Performance

These results were also as expected. An increase in relative humidity increases the power output from the PEMFC. This trend continued until the relative humidity set point temperature exceeded the operating temperature of the PEMFC, at which point a condensation event happened within the PEMFC due to the operating temperature being lower than the temperature of the humidified gas. Once the condensation event began, the PEMFC flooded at an increasing rate. As a result water built up over time on

the cathode side, which prevented the catalyst from processing the oxygen. As shown in Figure 17, prior to this flooding point, an increase in relative humidity caused an increase in the short circuit current and caused the I / V (current versus voltage) curve to become more linear (instead of exponentially decaying). The tests shown in Figure 17 were run using flow rates of 5ccm hydrogen and 50 ccm air, with a fixed PEMFC operating temperature of 65 ˚C and varying relative humidities.

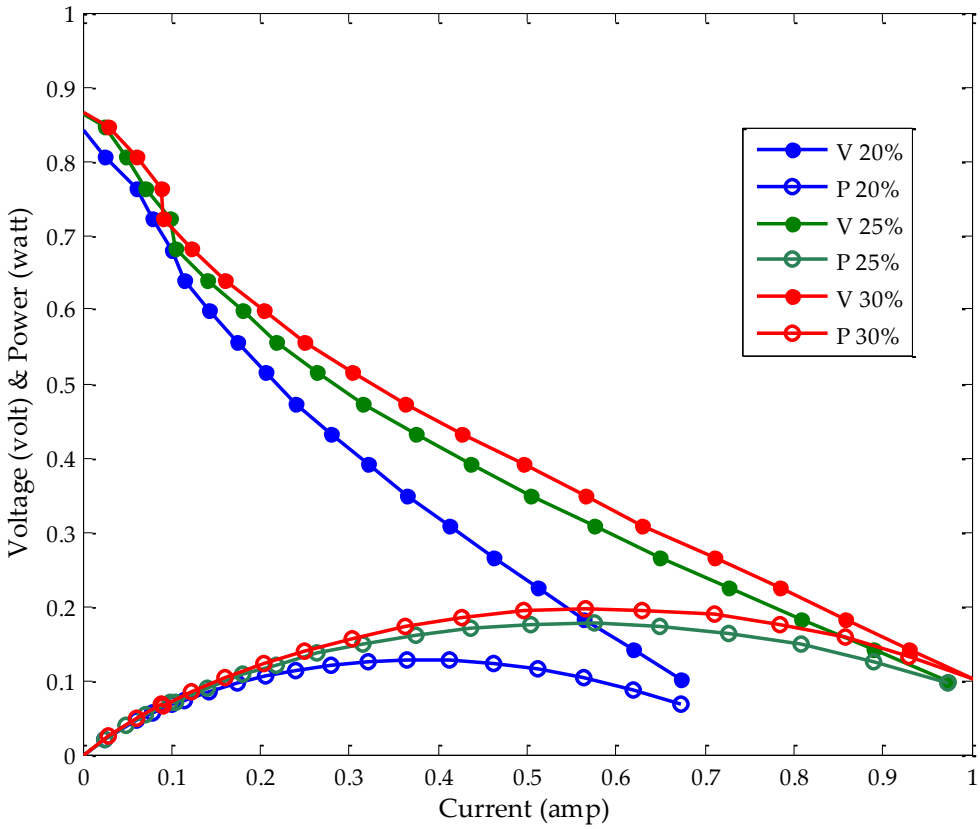

Figure 17: Effects of Relative Humidity

3.3 Finding the Optimal Operation Point

As already described, the two operating variables are coupled. If the relative humidity is increased, the fuel cell temperature should also be increased. The maximum power output performance occurred when the two temperatures matched. This matching is required because the PEMFC operating temperature causes dehydration of the membrane while the relative humidity causes flooding of the membrane. If the temperatures are balanced the negative effect of each is offset proportionally, leaving only the benefits of each of condition. Fuel cell temperatures were varied from 60 ˚C to 70 ˚C and relative humidity was varied from 15% to 35%, with additional spot checks above and below these ranges analyzed to ensure the correct ranges were being examined. The results in Figures 18 – 20 show that the optimal operation point for this PEMFC system is 70 ˚C operating temperature and 30% relative humidity. It was also determined that this optimal operation point varied somewhat between replacement membranes, but the trend of matching the two temperature settings continued and remained within a range of ±5 ˚C.

The present experiment showed that there was little increase in power at operating temperatures above 70 ˚C. While the maximum power did continue to increase, the stability of the power curve decreased proportionally (refer to fluctuation data shown in Figure 20). Therefore, it became harder to control the setup at temperatures above 70 ˚C. The goal was take all measurements at the optimal operation

point where the maximum power output from the PEMFC occurred, because any negative effects would be more dramatic at that point. The tests shown in Figure 19 were run using flow rates of 5ccm hydrogen and 50 ccm air.

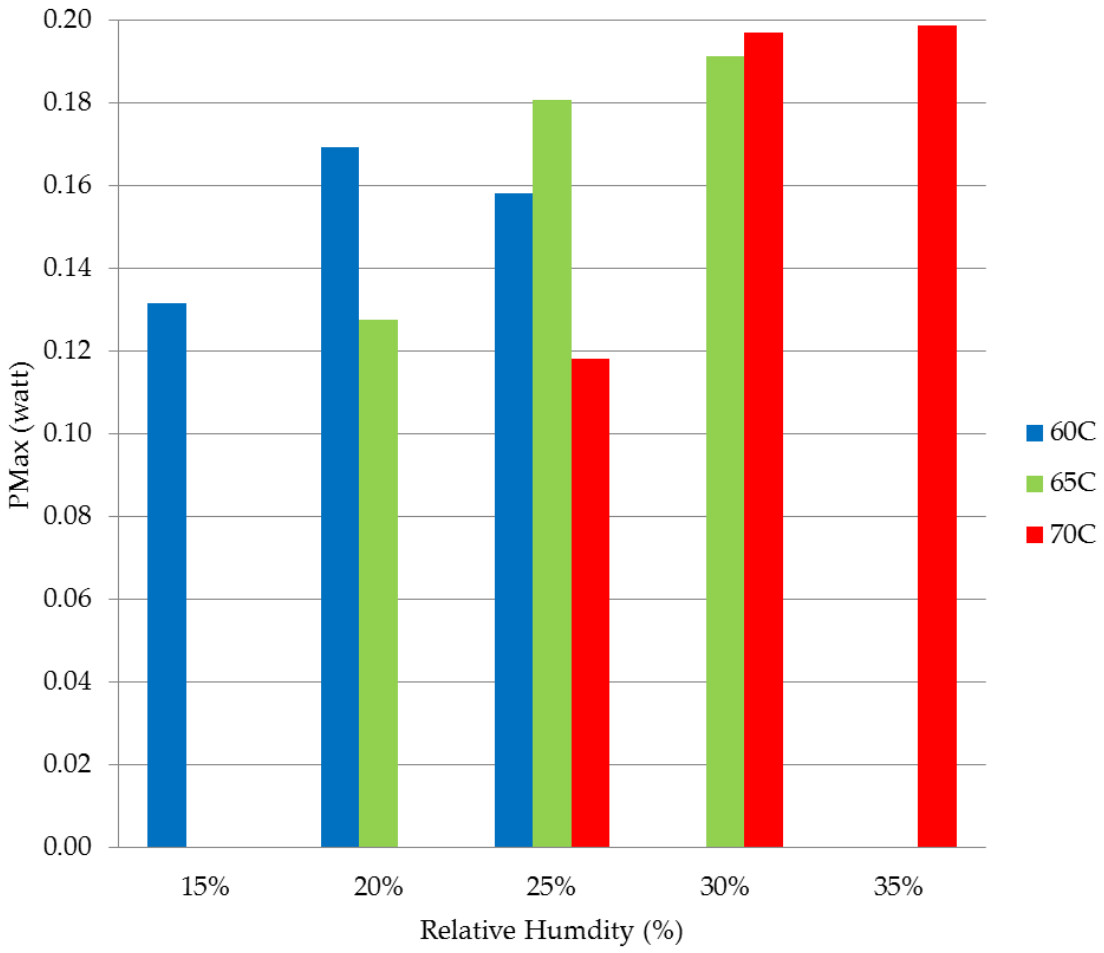

Figure 18: Average Maximum Power Analysis with Varying Input Conditions

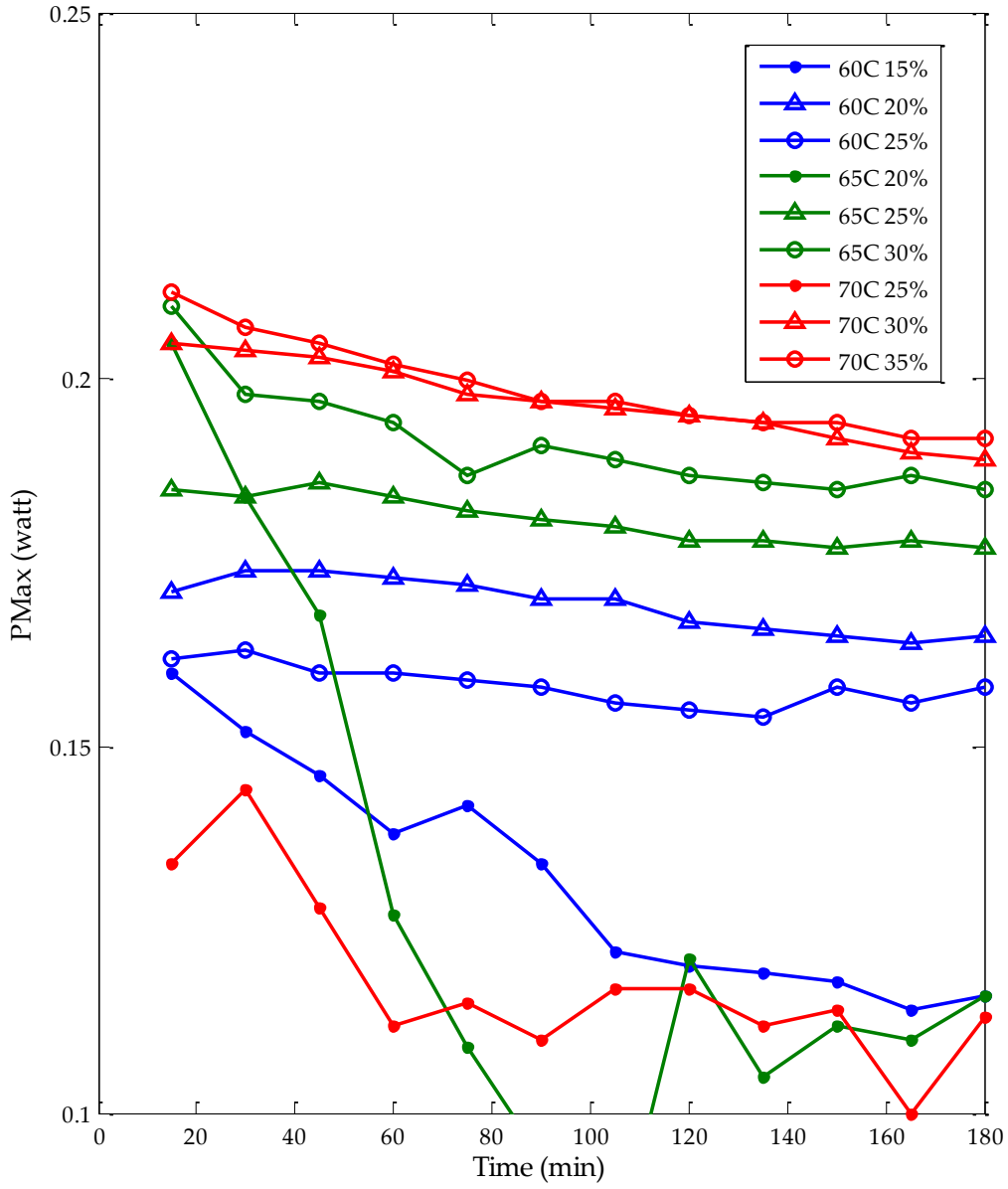

Figure 19: Power Curve Comparison with Varying Input Conditions

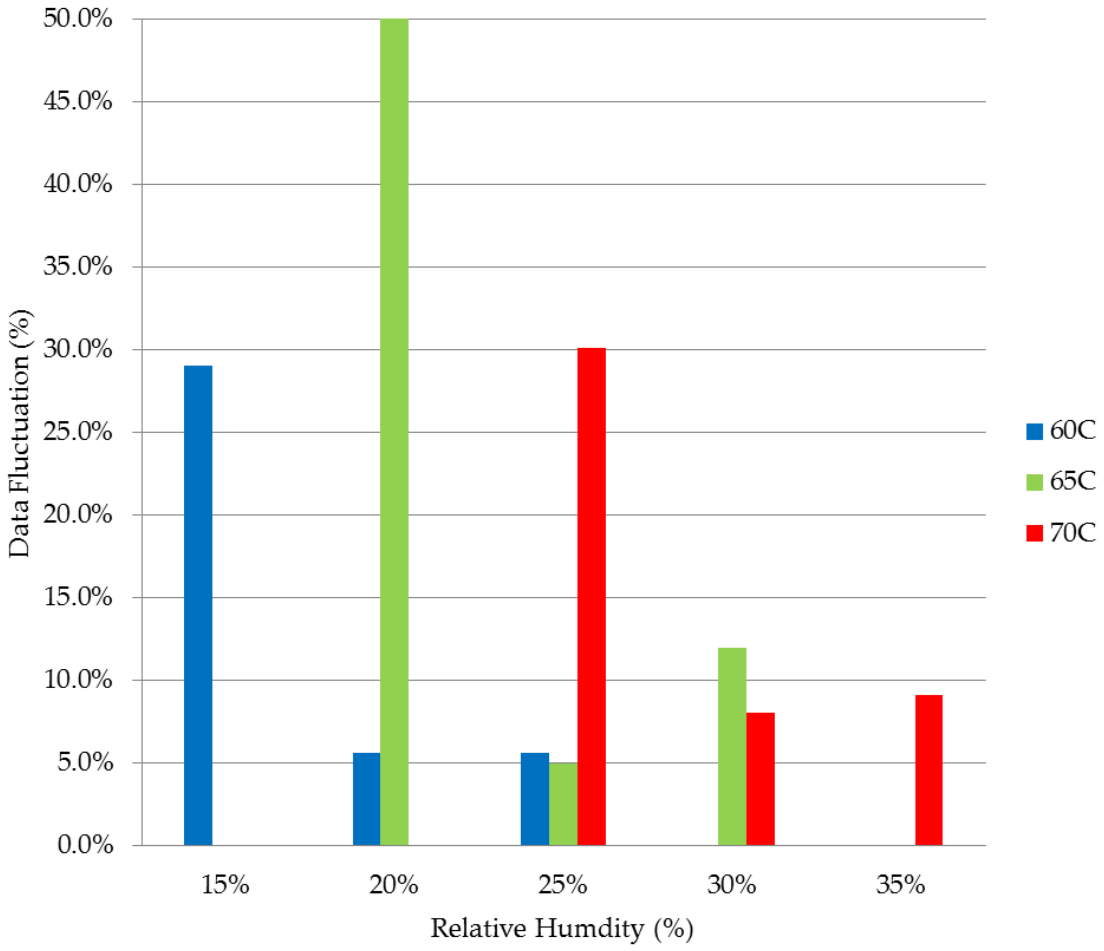

Figure 20: Data Fluctuation Comparisons

3.4 Effects of Carbon Dioxide on PEMFC Performance

The next set of experiments added carbon dioxide into the fuel mixture being directed into the anode side of the PEMFC. The carbon dioxide level in the fuel mixture was varied from 0% to 30%. The results shown in Figures 21 – 22 demonstrate that all

tested levels of carbon dioxide resulted in power curves within the normal operational range of the PEMFC (i.e. any effects from the carbon dioxide are negligible as regards this specific PEMFC). The power output when using a mixture containing 30% carbon dioxide resulted approximately in the same power output as when using pure hydrogen. However, the data did show that the higher the level of carbon dioxide within the mixture, the more likely that the resulting power curve will be on the lower end of the operational range of the PEMFC.

After all of the carbon dioxide runs were completed, an additional pure hydrogen run was performed to verify that no catalyst degradation had occurred due to carbon monoxide poisoning and all power levels were within acceptable ranges. It was therefore shown that carbon dioxide has no effect on this PEMFC and does not break down into carbon monoxide in this PEMFC. This finding indicates that if all of the carbon monoxide could be cleaned out of the expected gas mixture from the solar collector (75% H_2, 24% CO_2, 1% CO) by the PROX, the PEMFC would react as if it were pure hydrogen and therefore generate the appropriate power curve.

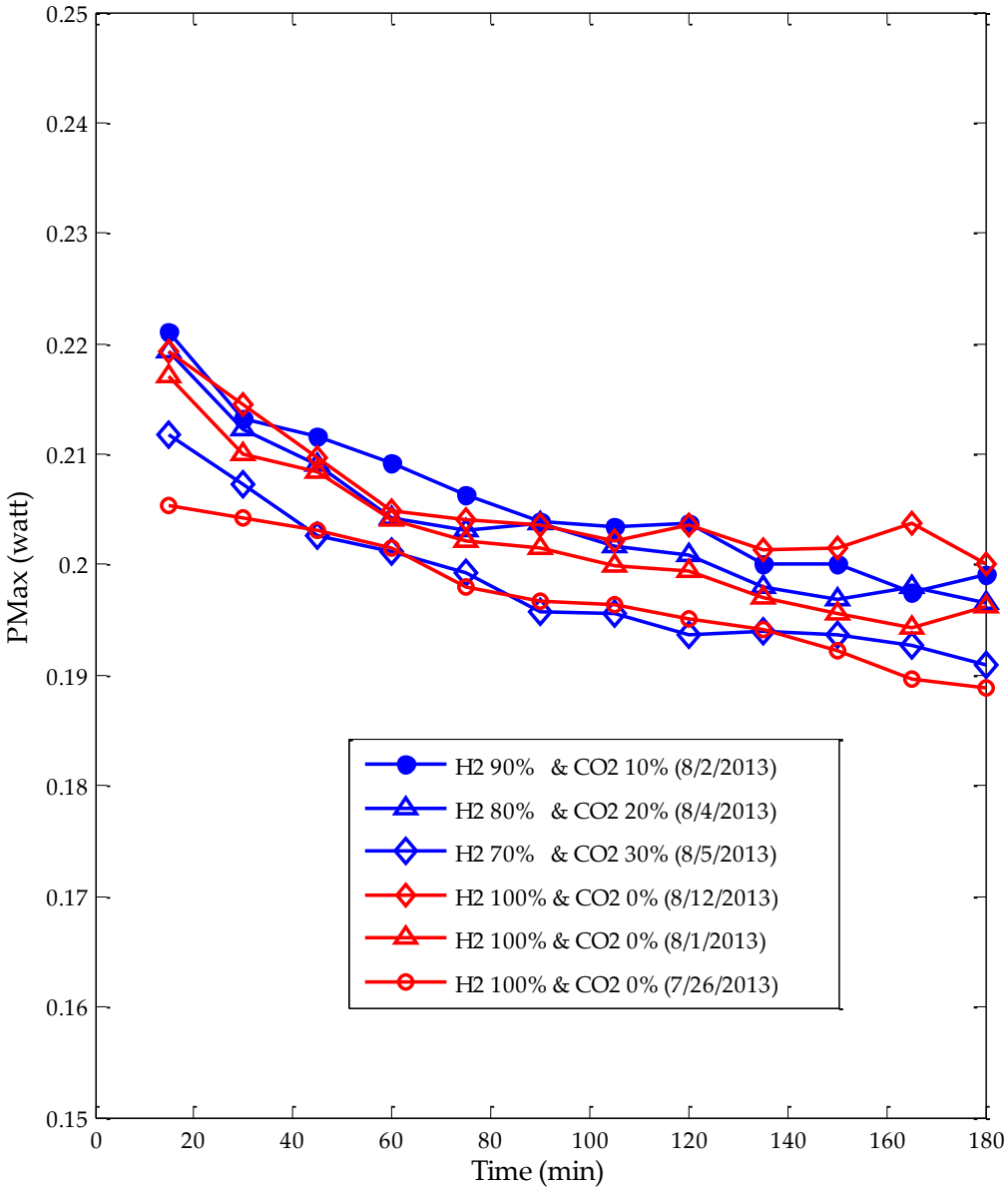

Figure 21: Power Curve Comparison with Varying Gas Mixture

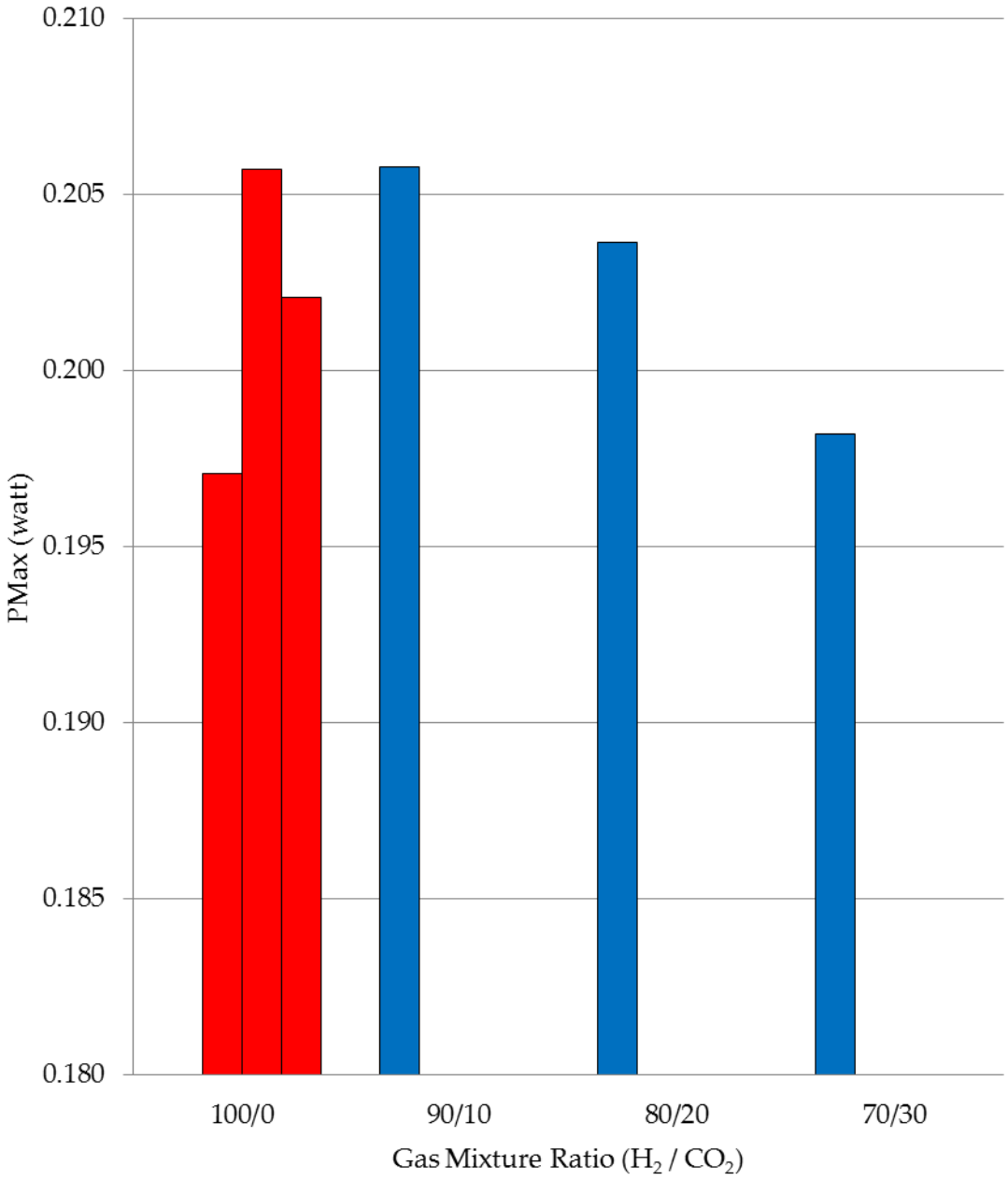

Figure 22: Average Maximum Power Analysis with Varying Gas Mixture

3.5 Effects of Carbon Monoxide and Carbon Dioxide on PEMFC Performance Using PROX

In the next set of experiments, the PROX was added to the setup as described in Section 2.9. Two runs were performed using the expected gas mixture as the input for the PROX and the clean mixture was then directed into the PEMFC. The first run yielded a lower power curve as compared to a pure hydrogen run. This power curve had an average power level of approximately 0.13 watts (as seen in Section 3.4, a pure hydrogen run produces approximately 0.20 watts). The second run caused the membrane to be poisoned by the carbon monoxide within 15 minutes. Both of these runs can be seen in Figure 23 below, with the third run providing confirmation of the carbon monoxide poisoning (by having a pure hydrogen mixture supplied to the PEMFC after the second run). The assumption is that small leaks in the setup during the first run caused the diminished power curve. The whole system was thoroughly checked for leaks before the second run was performed.

As shown below, at the start of the second run the power curve was consistent with expectations. However, the PROX did not achieve 100% conversion during this run, causing approximately 110 ppm of carbon monoxide to remain within the flow leading to the PEMFC. Unfortunately, this level of carbon monoxide far exceeded the threshold of 10 ppm and resulted in membrane poisoning within 15 minutes. The second run was stopped early (after 30 minutes) in an attempt to save the membrane; however this was found to be futile. Additional runs were planned after simply

replacing the poisoned membrane and using new PROX, but due to unrelated problems (with the controllers governing the heat wires) these runs have not yet been completed. Despite the result of the second run, if the PROX has a 100% conversion rate (as shown by Shodiya [28]), the PEMFC should perform as if the flow consisted of pure hydrogen (see Section 3.4).

In spite of the leaks and the poisoning, there are significant positive results from this experiment. The experiment established that future runs need to have the gas chromatograph data more strictly reviewed prior to the gas being allowed to enter the PEMFC. It was also found that the method of running the cleaned gas through the gas chromatograph for 60 minutes while sampling it in 15 minute intervals was not sufficiently effective. A longer duration and better analysis of the sampling data will solve these problems.

Another factor that could have contributed to the diminished power levels seen in the first run was the flow rate in and out of the PROX. This flow rate needs to be more carefully monitored to ensure the correct flow rate of hydrogen, because as discussed in Section 3.6 below, an increased hydrogen flow rate causes a lower power level.

Both of these issues have been addressed for future experiments, but continuing issues with the controllers have prevented further tests. A continued effort will be made to get further data until graduation. If no results have been gathered by then, the

experiment and knowledge of the setup will be turned over to Shodiya and others for further research.

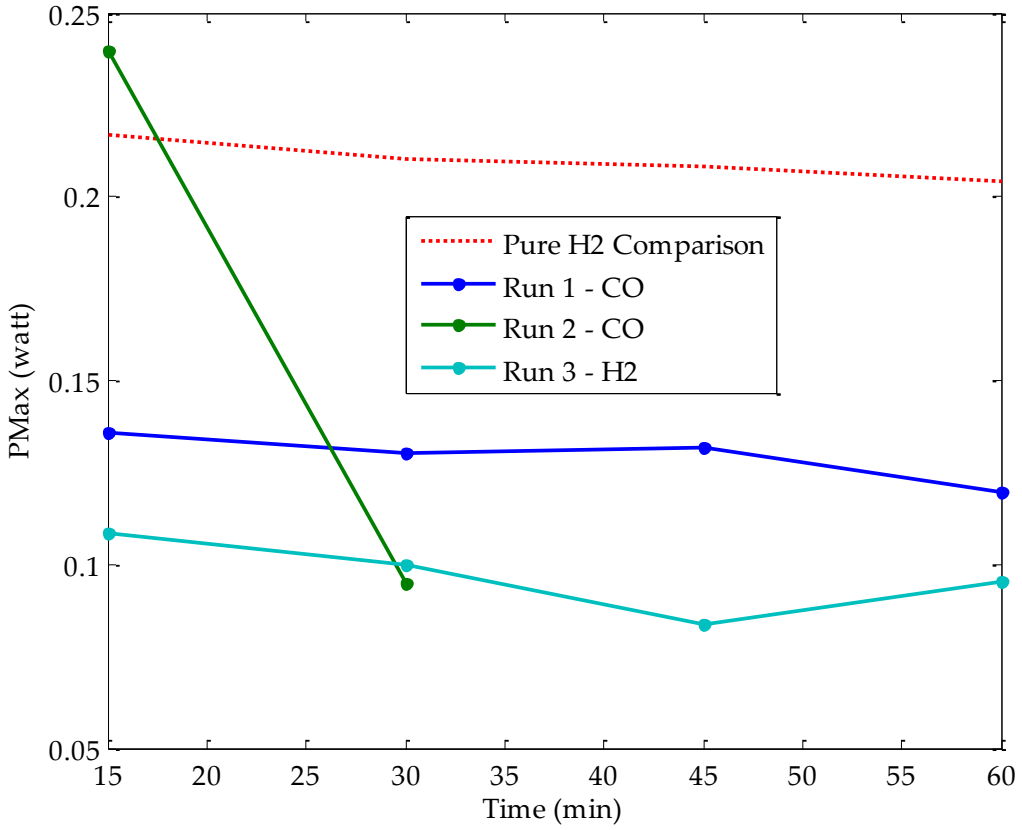

Figure 23: Power Curve Comparison with CO added using PROX

3.6 Other Findings

Three interesting discoveries were made with regard to the PEMFC during the course of the experiments. These discoveries were: quantifying the effects on maximum power output, both when the flow rate of hydrogen was varied and when multiple runs

of the experiment were attempted without allowing for a cool down period; and that when the membranes are replaced they produce low power levels for the first few runs.

The first unexpected result is shown in Figure 24, which demonstrates that slower flow rates increased the maximum power of the PEMFC. Note that in all of these tests the operating temperature of the PEMFC was 60 ˚C with a relative humidity of 20%, a constant air flow rate of 50 ccm, and a varying hydrogen flow rate. This result is counter-intuitive because one would assume that faster flow rates supply more hydrogen into the system, thus giving the platinum catalyst the opportunity to split more hydrogen. Based on the results seen in Figure 24, it could be hypothesized that the splitting action performed by the catalyst is a fragile process. The more energetic the flow, the less likely it is that the hydrogen will be split. Awareness of this flow rate issue is vital because if the gas mixture experiments (see Sections 3.4 and 3.5) are run at a fixed flow rate, the hydrogen flow rate within the gas mixture will decrease as the ratio of hydrogen to carbon dioxide increases as seen in Table 3 (to ensure there is absolutely no confusion, the flow rates in Table 3 are *not* what should be used in the experiment).

If the carbon dioxide experiment (seen in Section 3.4) is performed using the fixed flow rate found in Table 3 rather than the correct values seen in Table 2, the experiment will yield a result that shows that the maximum power will increase as carbon dioxide within the gas mixture increases, as seen in Figure 25. This inaccurate increase in power can be attributed to the decrease in hydrogen flow rate within the fuel.

Figure 24 shows that at lower flow rates of hydrogen there is an increased maximum power level. Therefore, running the experiments using fixed flow rates yields power curves that are not comparable to each other. Because this issue is likely to appear when the PROX is added to the system, the gas flow out of the PROX has to be carefully monitored to ensure that valid flow rates of hydrogen into the PEMFC remain stable so that the power curves can be compared.

Table 3: Fixed Mixture Gas Flow Rates

Gas Mixture	H_2 (ccm)	CO_2 (ccm)	Total Mixture (ccm)
100% H_2 0% CO_2	5.00	0.00	5.00
90% H_2 10% CO_2	4.50	0.50	5.00
80% H_2 20% CO_2	4.00	1.00	5.00
70% H_2 30% CO_2	3.50	1.50	5.00

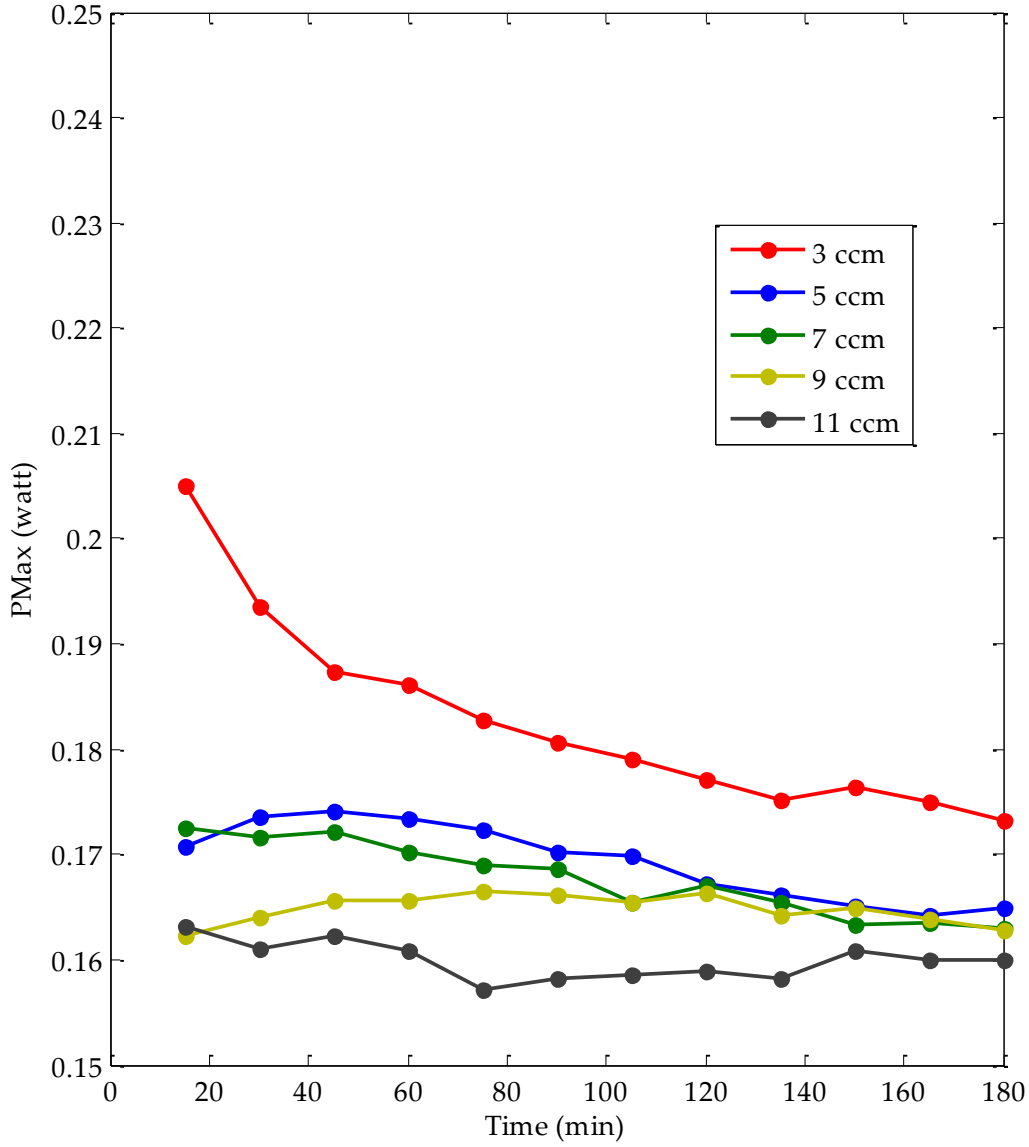

Figure 24: Power Curve Comparison with Varying Hydrogen Flow Rates

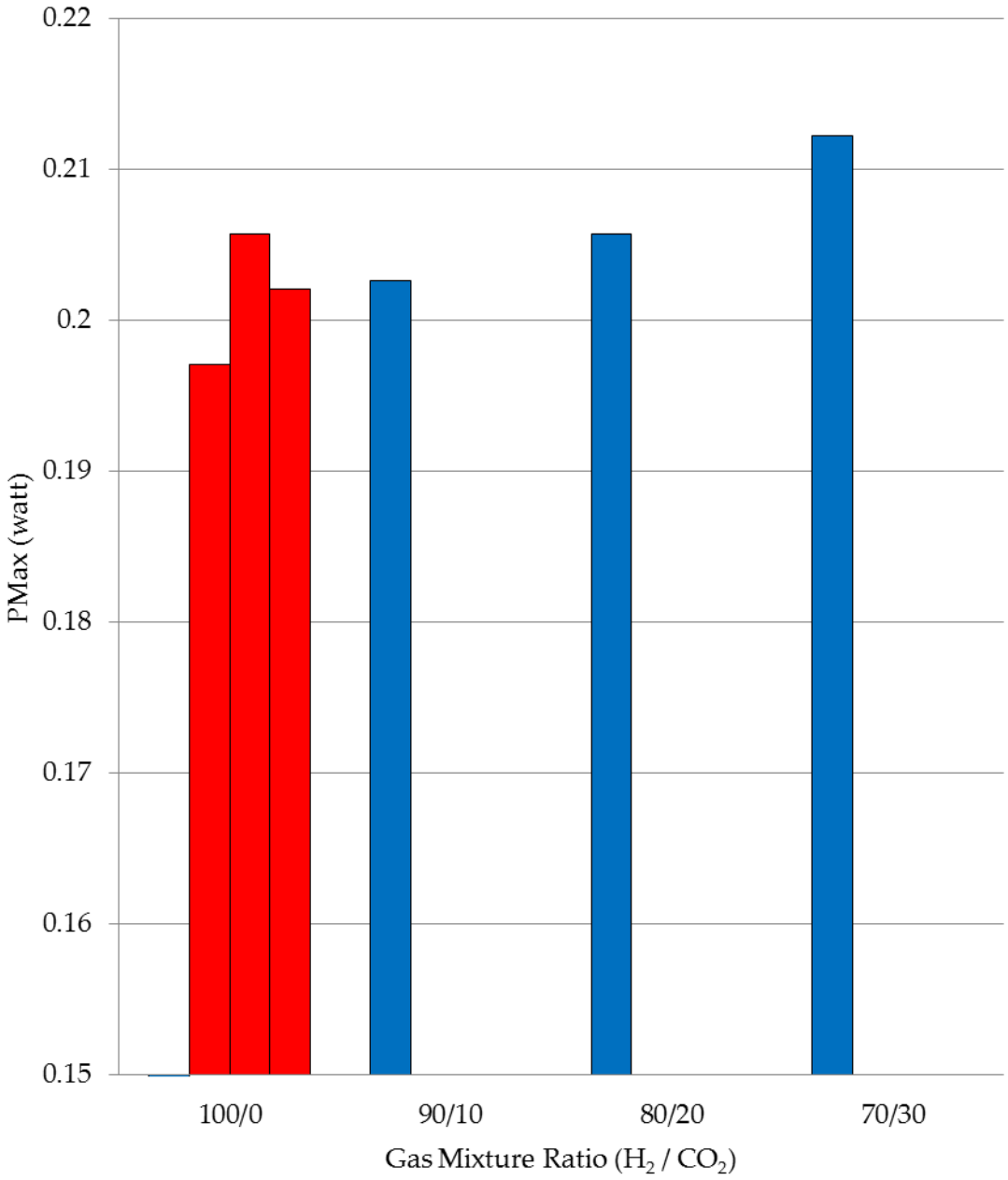

Figure 25: Carbon Dioxide Experiment with Fixed Flow Rate

The second unexpected finding is shown in Figure 25, which demonstrates that if multiple experiments were run back to back then the second of the two runs yielded an

inaccurate lower maximum power level. This inaccuracy is directly related to the slightly negative slope associated with the setup (discussed in Section 2.6). This finding helped to explain the slow flooding issue that caused the slightly negative slope and prevented the ability to compare the power curves.

To examine this issue, two sets of two runs were performed with the time between individual runs varied. During this down time, dry nitrogen gas (inert) was run through the system to facilitate the removal of any excess water. It was found that unless nitrogen was run through the system, only one run could be performed each day as the system needed to cool down and dry out overnight. If it were necessary to complete two runs in the same day, nitrogen would need to be run through the system for 30 to 45 minutes. Any shorter nitrogen duration would not remove enough water, while any longer nitrogen duration would dehydrate the membrane. Figure 26 shows the results of two sets of two runs in which the down time (with nitrogen flowing) was varied from 30 to 60 minutes.

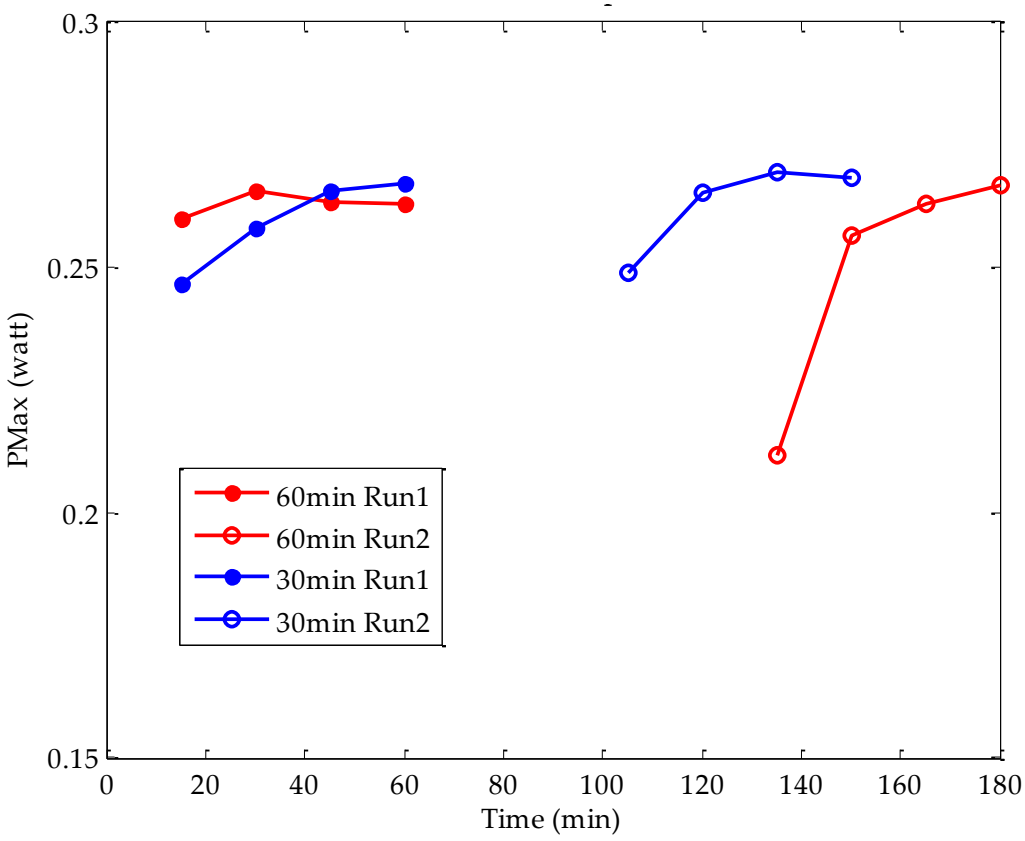

Figure 26: Power Curve Comparison with Varying Down Time with Nitrogen Flowing

The third and final interesting result observed was that when the membrane is replaced within the PEMFC, power levels were lower for about three to five runs. A logical assumption is that a coating of some kind was added to the membrane prior to shipping, which takes time to either decay or to be removed from the membrane by the gas flow. After this initial "break-in" period, the power levels stabilized and yielded consistent results.

4. Conclusion

Overall, the series of experiments was successful. It validated the concept of the HSS. A PEMFC setup was designed and constructed that produced a stable power curve over the course of a 3- hour run. This setup allowed verification of the effects of varying both the operating temperature of the PEMFC and the relative humidity. Using this setup, the experiment proved that even if the gas mixture input to the PEMFC consisted of 30% carbon dioxide and 70% hydrogen, the PEMFC would continue to operate as if the flow were 100% hydrogen with no negative long term effects to the PEMFC. The PROX was then added to the setup and the expected gas mixture (from the solar collector) was run through the system. While the actual results were not ideal, they clearly demonstrate that if the PROX achieves the expected 100% conversion (removal of the carbon monoxide to the necessary level of < 10 ppm) the PEMFC should handle the expected cleaned flow as if it were 100% hydrogen.

4.1 Future Recommended Setup Revisions

Although the current setup works well and performs the desired tasks, a few revisions would be beneficial to reduce the overall maintenance issues still plaguing the system.

The first and most critical weak point of the system is the Parafilm used to seal the corks of the boilers. The Parafilm melts if the heat wire gets too hot, and therefore loses its ability to create an air tight seal. It should be removed and replaced with a

temperature resistant sealant. The only reason the Parafilm currently remains in the setup is to provide the ability to completely take apart the boilers and tubing for cleaning.

The next weak point is the plastic tubing used in the conveyance lines. This tubing should be replaced with metal pipe that would provide higher thermal conductivity. This would result in more effective heating of the gas within the conveyance lines by making the heat more uniform and increasing the conveyance lines' ability to store the heat, which would result in fewer heat losses. Therefore, this change could possibly allow for reduction in the number of heat wires and in their size. The plastic tubing has remained in the setup because the tubing is transparent, allowing for easy diagnosis of any condensation issues. The plastic tubing has a major safety concern, which is that like the Parafilm previously discussed, if the heat wires get too hot the tubing will melt and create a gas leak within the lab. Metal pipe would solve this issue because the material would withstand the high temperatures that the heat wire can generate.

References

1. Bejan, A., & Lorente, S. (2008). *Design with constructal theory* (pp. 1-164 & 467-490). Hoboken, N.J: John Wiley & Sons.

2. Vishnyakov, V. M. (2006). Proton exchange membrane fuel cells. *Vacuum, 80*(10), 1053-1065. doi:10.1016/j.vacuum.2006.03.029

3. Barbir, F. (2013). *PEM fuel cells theory and practice: Theory and practice* (pp. 1-158 & 265-371). Amsterdam: Elsevier/Academic Press.

4. Xia, Y., Yangiu, Z., & Zhuxian, Y. (2013). Porous carbon-based materials for hydrogen storage: Advancement and challenges. *Journal of Materials Chemistry A, 1*(33), 9365-9381. doi:10.1039/c3ta10583k

5. Panagiotopoulou, P., Papadopoulou, C., Matralis, H., & Verykios, X. (2013; 2013). Production of renewable hydrogen by reformation of biofuels *Wiley Interdisciplinary Reviews: Energy and Environment,* doi:10.1002/wene.93

6. Mohapatra, S. (2012). Hydrogen Production Technologies with Specific Reference to Biomass *Internal Journal of Renewable Energy Research*, 2(3), from http://www.ijrer.org/index.php/ijrer/article/viewFile/245/pdf

7. van de Krol, R., Liang, Y., & Schoonman, J. (2008). Solar hydrogen production with nanostructured metal oxides. *Journal of Materials Chemistry, 18*(20), 2311-2320. doi:10.1039/b718969a

8. Saxena, S., Kumar, S., & Drozd, V. (2011). A modified steam-methane-reformation reaction for hydrogen production. *International Journal of Hydrogen Energy, 36*(7), 4366-4369. doi:10.1016/j.ijhydene.2010.12.133

9. Fabian, T., O'Hayre, R., Litster, S., Prinz, F. B., & Santiago, J. G. (2010). Passive water management at the cathode of a planar air-breathing proton exchange membrane fuel cell. *Journal of Power Sources, 195*(10), 3201-3206. doi:10.1016/j.jpowsour.2009.12.030

10. Owejan, J. P., Gagliardo, J. J., Sergi, J. M., Kandlikar, S. G., & Trabold, T. A. (2009). Water management studies in PEM fuel cells, part I: Fuel cell design and in situ water distributions. *International Journal of Hydrogen Energy, 34*(8), 3436-3444. doi:10.1016/j.ijhydene.2008.12.100

11. Lu, Z., Kandlikar, S. G., Rath, C., Grimm, M., Domigan, W., White, A. D., Hardbarger, M., Owejan, J.P., Trabold, T. A. (2009). Water management studies in PEM fuel cells, part II: Ex situ investigation of flow maldistribution, pressure drop and two-phase flow pattern in gas channels. *International Journal of Hydrogen Energy, 34*(8), 3445-3456. doi:10.1016/j.ijhydene.2008.12.025

12. Lu, Z., Daino, M. M., Rath, C., & Kandlikar, S. G. (2010). Water management studies in PEM fuel cells, part III: Dynamic breakthrough and intermittent drainage characteristics from GDLs with and without MPLs. *International Journal of Hydrogen Energy, 35*(9), 4222-4233. doi:10.1016/j.ijhydene.2010.01.012

13. Cheng, X., Shi, Z., Glass, N., Zhang, L., Zhang, J., Song, D., Zhong-Sheng, L., Wang, H., Shen, J. (2007). A review of PEM hydrogen fuel cell contamination: Impacts, mechanisms, and mitigation. *Journal of Power Sources, 165*(2), 739-756. doi:10.1016/j.jpowsour.2006.12.012

14. Divisek, J., Oetjen, H. -F., Peinecke, V., Schmidt, V. M., & Stimming, U. (1998). Components for PEM fuel cell systems using hydrogen and CO containing fuels. *Electrochimica Acta, 43*(24), 3811-3815. doi:10.1016/S0013-4686(98)00140-6

15. Qi, Z., He, C., & Kaufman, A. (2002). Effect of CO in the anode fuel on the performance of PEM fuel cell cathode. *Journal of Power Sources, 111*(2), 239-247. doi:10.1016/S0378-7753(02)00300-2

16. Janssen, G.J.M., Lebedeva, N.P., (2004). Carbon Dioxide Poisoning on Proton-Exchange-Membrane Fuel Cell Anodes. Paper presented at Fuel Cells Science and Technology (ECN-RX—05-073), Munich, Germany, *ECN energy innovation*. from http://www.ecn.nl/docs/library/report/2005/rx05073.pdf

17. de Bruijn, F. A., Papageorgopoulos, D. C., Sitters, E. F., & Janssen, G. J. M. (2002). The influence of carbon dioxide on PEM fuel cell anodes. *Journal of Power Sources, 110*(1), 117-124. doi:10.1016/S0378-7753(02)00227-6

18. Gu, T., Lee, W. -K., & Zee, J. W. V. (2005). Quantifying the 'reverse water gas shift' reaction inside a PEM fuel cell. *Applied Catalysis B, Environmental, 56*(1), 43-50. doi:10.1016/j.apcatb.2004.08.016

19. Janssen, G. J. M. (2004). Modelling study of CO_2 poisoning on PEMFC anodes. *Journal of Power Sources, 136*(1), 45-54. doi:10.1016/j.jpowsour.2004.05.004

20. Hotz, N. (2012). Hybrid solar system for decentralized electric power generation and storage. *Journal of Solar Energy Engineering, 134*(4), 41010.

21. Sonntag, R. E., Borgnakke, C. Van Wylen, G. J. V. (2003). *Fundamentals of thermodynamics* (pp. 40-272). New York: Wiley.

22. Reid, R. C., Prausnitz, J. M., & Poling, B. E. (1987). *The properties of gases and liquids* (pp. 208-212). New York: McGraw-Hill.

23. Zhang, J., Zhang, J., Tang, Y., Song, C., Xia, Z., Li, H., & Wang, H. (2008). PEM fuel cell relative humidity (RH) and its effect on performance at high temperatures. *Electrochimica Acta, 53*(16), 5315-5321. doi:10.1016/j.electacta.2008.02.074

24. Pérez-Page, M., & Pérez-Herranz, V. (2011). Effects of the Operation and Humidification Temperatures on the Performance of a Pem Fuel Cell Stack on Dead-End Mode. *International Journal of Electrochemical Science*, 6, 492-505. from http://www.electrochemsci.org/papers/vol6/6020492.pdf

25. Yan, Q., Toghiani, H., & Causey, H. (2006). Steady state and dynamic performance of proton exchange membrane fuel cells (PEMFCs) under various operating conditions and load changes. *Journal of Power Sources, 161*(1), 492-502. doi:10.1016/j.jpowsour.2006.03.077

26. Wang, L., Husar, A., Zhou, T., & Liu, H. (2003). A parametric study of PEM fuel cell performances. *International Journal of Hydrogen Energy, 28*(11), 1263-1272. doi:10.1016/S0360-3199(02)00284-7

27. Cussler, E. L. (2009). *Diffusion mass transfer in fluid systems: Mass transfer in fluid systems* (pp. 237-455). Cambridge: Cambridge University Press.

28. Shodiya T., Schmidt O., Peng W., & Hotz N. (2013). Novel nano-scale Au/α-Fe_2O_3 catalyst for the preferential oxidation of CO in biofuel reformate gas. *Journal of Catalysis, 300*, 63-69. doi:10.1016/j.jcat.2012.12.027

29. ElectroChem, Inc. *Schematic of ElectroChem's Fuel Cell Hardware Components*, n.d., Retrieved March 9, 2014, from http://fuelcell.com/fuel-cell-hardware/

30. Grove WR. (1842). On a Gaseous Voltaic Battery. *London and Edinburgh Philosophical Magazine and Journal of Science*. 21(Series 3):417-20.